Titanium(II), -(III), and -(IV) Complexes Supported by Benzamidinate Ligands

John R. Hagadorn and John Arnold*

Department of Chemistry, University of California, Berkeley, California 94720-1460

Received October 27, 1997

The synthesis and reactivity of a wide range of titanium benzamidinates is described. Addition of 0.5 equiv of Me_2Mg to the dichloride L_2TiCl_2 (L = $PhC(NSiMe_3)_2$) in Et_2O yields the chloro−alkyl derivative $L_2Ti(Me)Cl$ in good yield. The addition of 2 equiv of $PhCH_2MgCl$ to the dichloride affords thermally sensitive $L_2Ti(CH_2Ph)_2$ in moderate yield. Likewise, addition of 1 equiv of Me_2Mg results in the clean formation of the dimethyl L_2TiMe_2. The dimethyl reacts with *tert*-butylamine in refluxing benzene to form the five-coordinate imido $L_2TiNCMe_3$, for which crystallographic data is presented. The imido reacts with acetone in C_6D_6 to form the bridging oxo derivative $L_2Ti(\mu\text{-}O)_2TiL[\eta^1\text{-}NC(Ph)N(SiMe_3)_2]$. Overnight reduction of the dichloride with 1% Na/Hg amalgam in tetrahydrofuran (THF) forms the Ti(III) derivative $L_2TiCl(THF)$, which is crystallized from hexanes in moderate yield. Carrying out the analogous reduction in toluene yields the base-free Ti(III) chloride, L_2TiCl, for which crystallographic data is presented. Allowing the reaction (in toluene) to proceed for an additional 48 h results in further reduction and the formation of the end-on bound dinitrogen complex $(L_2Ti)_2(\mu\text{-}N_2)$, which is isolated as dark blue crystals from hexanes in moderate yield. Reduction of $L_2Ti(Me)Cl$ with 1% Na/Hg amalgam in THF forms the Ti(III) methyl derivative which is isolated as the five-coordinate THF-free product L_2TiMe upon evacuation and crystallization from hexamethyldisiloxane (HMDSO). The related Ti(III) alkyl $L_2TiCH_2SiMe_3$ is readily prepared by reaction of $LiCH_2SiMe_3$ with L_2TiCl in toluene. Carrying out the 1% Na/Hg amalgam reduction of the dichloride in the presence of CO results in the formation of the Ti(III) bridging-oxo species $(L_2Ti)_2(\mu\text{-}O)$, which is isolated in low yield. CO as the sole oxygen source is confirmed by the use of $C^{18}O$, which yielded only labeled product. Analogous reduction in the presence of *N*,*N*,*N*′,*N*′-tetramethylethylenediamine (TMEDA) results in the C−N bond cleavage of an amidinate ligand and the cyclometalation of TMEDA. Two products, $L_2TiNSiMe_3$ and $LTi[\eta^2\text{-}Me_3SiNC(H)Ph][\eta^3\text{-}CH_2N(Me)CH_2CH_2NMe_2]$, are isolated in good yields by fractional crystallization from hexanes. The dinitrogen complex, $(L_2Ti)_2(\mu\text{-}N_2)$, reacts with pyridine (Py) and 2,6-dimethylphenyl isocyanide (XylylNC) to form base adducts $[L_2Ti(Py)]_2(\mu\text{-}N_2)$ and $[L_2Ti(CNXylyl)]_2(\mu\text{-}N_2)$ without loss of the dinitrogen ligand. Crystallographic data for the Py adduct is presented. Oxidation reactions of $(L_2Ti)_2(\mu\text{-}N_2)$ with a variety of oxygen and sulfur sources is reported. Reaction with dry O_2 in the presence of pyridine gives the seven-coordinate peroxo complex $L_2Ti(\eta^2\text{-}O_2)Py$. The related reaction with excess S_8 yields the dark-green persulfido derivative $L_2Ti(\eta^2\text{-}S_2)$, for which crystallographic data is presented. The persulfido reacts overnight with Hg in toluene solution to give the bimetallic sulfido complex $L_2Ti(\mu\text{-}S)_2TiL[\eta^1\text{-}NC(Ph)N(SiMe_3)_2]$, which is formed following a silyl-group migration. The analogous oxygen-containing product is best prepared by the reaction of powdered $(L_2Ti)(\mu\text{-}N_2)$ with dry O_2. In the presence of excess pyridine, $L_2Ti(\eta^2\text{-}S_2)$ reacts with Hg to yield the terminal sulfido $L_2Ti(S)Py$. The crystallographically characterized terminal-oxo derivative $L_2Ti(O)OPy$ is prepared by reaction of $(L_2Ti)(\mu\text{-}N_2)$ with an excess of pyridine *N*-oxide in toluene−pyridine.

Introduction

In recent years, there has been considerable effort put forth in developing supporting ligands in transition-metal chemistry, with a major goal being the tailoring of chemical reactivity and properties.[1,2] For monomeric transition-metal derivatives, supporting ligands are generally bulky in order to provide adequate steric shielding for the prevention of unwanted bimolecular reactivity and must provide the necessary electronic stabilization to the metal center. Studies utilizing a wide range of ligands have confirmed the influence of the ancillary ligand environment on reactivity, but the accurate prediction of reactivity from the structure remains a challenging problem. For the group 4 triad,

(1) Cotton, F. A.; Wilkinson, G. *Advanced Inorganic Chemistry,* 5th ed.; Wiley: New York, 1988.
(2) Elschenbroich, C.; Salzer, A. *Organometallics, A Concise Introduction,* 2nd ed.; VCH: Weinheim, 1992.

S0276-7333(97)00933-3 CCC: $15.00
Publication on Web 03/05/1998

Scheme 1

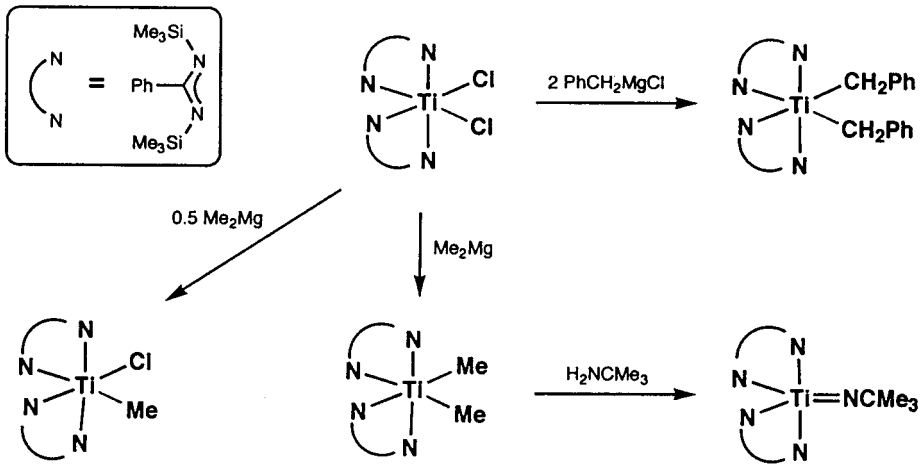

much of this research has been fundamental in nature but recently intense effort has been focused on complexes which serve as precursors to olefin polymerization catalysts. Toward these ends, complexes incorporating N-donor ligands such as amidos[3−13] and N_4-macrocycles[14−20] have shown considerable promise.

We are interested in the use of amidinate ligands in transition-metal chemistry. In the course of our studies, we have explored several general classes of amidinate systems including linked bis(amidinates)[21] and ferrocene-containing derivatives.[22] Here, we report chemistry that deals exclusively with the *N*,*N*′-bis(trimethylsilyl)benzamidinate (BTBA) ligand.[23] We found its use particularly attractive because as the ligand is prepared easily and cheaply on a large scale, its complexes are nicely soluble and generally highly crystalline and the ligand displays excellent NMR spectroscopic properties. Well-characterized BTBA complexes are known for a wide range of transition metals in various oxidation states across the periodic table. For titanium, a pair of Ti(IV) chloride derivatives were first reported in 1988 by Roesky[24] and Dehnicke.[25] Since then several workers have utilized these ligands for the stabilization of olefin polymerization catalysts,[26−30] some containing mixed cyclopentadienyl−amidinate ligand arrays.[31−33] Other workers have studied low-valent derivatives[34,35] and imidos[36] and have shown the utility of μ-formamidinate ligands for the preparation of complexes containing dititanium cores.[35,37] Here, we present our studies of Ti(IV) alkyl and imido derivatives, the reduction chemistry of L_2TiCl_2 leading to a variety of bond cleavages, and the reactivity of a dinitrogen complex with Lewis-bases and oxygen/sulfur sources. Portions of this work were communicated in preliminary reports.[38−40]

Results and Discussion

Alkyl and Imido Derivatives. The starting material for our investigations presented here is the Ti(IV) dichloride L_2TiCl_2, which was first synthesized and

(3) Burger, V. H.; Wiegel, K. *Z. Anorg. Allg. Chem.* **1973**, *398*, 257.
(4) Andersen, R. A. *Inorg. Chem.* **1979**, *18*, 2928.
(5) Planalp, R. P.; Andersen, R. A.; Zalkin, A. *Organometallics* **1983**, *2*, 16.
(6) Shapiro, P. J.; Cotter, W. D.; Schaefer, W. P.; Labinger, J. A.; Bercaw, J. E. *J. Am. Chem. Soc.* **1994**, *116*, 4623.
(7) Aoyagi, K.; Gantzel, P. K.; Kalai, K.; Tilley, T. D. *Organometallics* **1996**, *15*, 923.
(8) Cloke, F. G. N.; Geldbach, T. J.; Hitchcock, P. B.; Love, J. B. *J. Organomet. Chem.* **1996**, *506*, 343.
(9) Schaller, C. P.; Cummins, C. C.; Wolczanski, P. T. *J. Am. Chem. Soc.* **1996**, *118*, 591.
(10) Schrock, R. R.; Cummins, C. C.; Wilhelm, T.; Lin, S.; Reid, S. M.; Kol, M.; Davis, W. M. *Organometallics* **1996**, *15*, 1470.
(11) Scollard, J. D.; McConville, D. H. *J. Am. Chem. Soc.* **1996**, *118*, 10008.
(12) Warren, T. H.; Schrock, R. R.; Davis, W. M. *Organometallics* **1996**, *15*, 562.
(13) Tsuie, B.; Swenson, D. C.; Jordan, R. F.; Petersen, J. L. *Organometallics* **1997**, *16*, 1392.
(14) Goedken, V. L.; Ladd, J. A. *J. Chem. Soc., Chem. Commun.* **1982**, 142.
(15) Cotton, F. A.; Czuchajowska, J. *Polyhedron* **1990**, *9*, 2553.
(16) Housmekerides, C. E.; Ramage, D. L.; Kretz, C. M.; Shontz, J. T.; Pilato, R. S.; Geoffroy, G. L.; Rheingold, A. L.; Haggerty, B. S. *Inorg. Chem.* **1992**, *31*, 4453.
(17) Brand, H.; Arnold, J. *Angew. Chem., Int. Ed. Engl.* **1994**, *33*, 95.
(18) Brand, H.; Arnold, J. *Coord. Chem. Rev.* **1995**, *140*, 137.
(19) Giannini, L.; Solari, E.; De Angelis, S.; Ward, T. R.; Floriani, C.; Chiesi-Villa, A.; Rizzoli, C. *J. Am. Chem. Soc.* **1995**, *117*, 5801.
(20) Scott, M. J.; Lippard, S. J. *J. Am. Chem. Soc.* **1997**, *119*, 3411.
(21) Hagadorn, J. R.; Arnold, J. *Angew. Chem., Int. Ed. Engl.*, in press.
(22) Hagadorn, J. R.; Arnold, J. *Inorg. Chem.* **1997**, *36*, 132.
(23) For reviews of transition-metal amidinates, see: Edelmann, F. T. *Coord. Chem. Rev.* **1994**, *137*, 403. Dehnicke, K. *Chem.-Ztg.* **1990**, *114*, 295. Barker, J.; Kilner, M. *Coord. Chem. Rev.* **1994**, *133*, 219.
(24) Roesky, H. W.; Meller, B.; Noltemeyer, M.; Schmidt, H. G.; Scholz, U.; Sheldrick, G. M. *Chem. Ber.* **1988**, *121*, 1403.
(25) Fenske, D.; Hartmann, E.; Dehnicke, K. *Z. Naturforsch.* **1988**, *43b*, 1611.
(26) For Al-based ethylene polymerization catalysts supported by amidinates, see: Coles, M. P.; Jordan, R. F. *J. Am. Chem. Soc.* **1997**, *119*, 8125.
(27) Flores, J. C.; Chien, J. C. W.; Rausch, M. D. *Organometallics* **1995**, *14*, 1827.
(28) Flores, J. C.; Chien, J. C. W.; Rausch, M. D. *Organometallics* **1995**, *14*, 2106.
(29) Herskovicskorine, D.; Eisen, M. S. *J. Organomet. Chem.* **1995**, *503*, 307.
(30) Walther, D.; Fischer, R.; Gorls, H.; Koch, J.; Schweder, B. *J. Organomet. Chem.* **1996**, *508*, 13.
(31) Chernega, A. N.; Gomez, R.; Green, M. L. H. *J. Chem. Soc., Chem. Commun.* **1993**, 1415.
(32) Gomez, R.; Green, M. L. H.; Haggitt, J. L. *J. Chem. Soc., Chem. Commun.* **1994**, 2607.
(33) Gomez, R.; Duchateau, R.; Chernega, A. N.; Teuben, J. H.; Edelmann, F. T.; Green, M. L. H. *J. Organomet. Chem.* **1995**, *491*, 153.
(34) Dick, D. G.; Duchateau, R.; Edema, J. H.; Gambarotta, S. *Inorg. Chem.* **1993**, *32*, 1959.
(35) Cotton, F. A.; Wojtczak, W. A. *Polyhedron* **1994**, *13*, 1337.
(36) Stewart, P. J.; Blake, A. J.; Mountford, P. *Inorg. Chem.* **1997**, *36*, 3616.
(37) Hao, S. K.; Feghali, K.; Gambarotta, S. *Inorg. Chem.* **1997**, *36*, 3390.
(38) Hagadorn, J. R.; Arnold, J. *Organometallics* **1994**, *13*, 4670.
(39) Hagadorn, J. R.; Arnold, J. *J. Am. Chem. Soc.* **1996**, *118*, 893.
(40) Hagadorn, J. R.; Arnold, J. *Inorg. Chem.* **1997**, *36*, 2928.

structurally characterized by Roesky.[24] We have found that its synthesis is most conveniently carried out by the addition of (TMEDA)LiL to $TiCl_4(THF)_2$ in THF, as described by Gambarotta,[34] followed by crystallization from CH_2Cl_2. As shown in Scheme 1, the preparation of Ti(IV) alkyl derivatives from L_2TiCl_2 is readily accomplished by salt-metathesis reactions with Grignard and dialkylmagnesium reagents. The monoalkyl derivative $L_2Ti(Me)Cl$ was readily prepared by the slow addition of 0.5 equiv of Me_2Mg to a clear orange-red benzene solution of L_2TiCl_2. Removal of volatile materials from the red solution and crystallization from CH_2Cl_2 gave the product as dark red crystals in 72% yield. When the reaction was carried out in Et_2O with 1 equiv of Me_2Mg, complete conversion to L_2TiMe_2 occurred and the product was crystallized from CH_2Cl_2 in 60% yield. The dibenzyl derivative $L_2Ti(CH_2Ph)_2$ was prepared by the addition of $PhCH_2MgCl$ to a toluene solution of L_2TiCl_2 at −78 °C. The product was isolated as dark purple crystals from Et_2O in 44% yield. C_6D_6 solutions of the dibenzyl are thermally sensitive, decomposing within hours at 45 °C with the formation of toluene. Compared to the dibenzyl, both methyl derivatives are thermally stable in solution. Additionally, as solids, they are stable for at least 1 year in a fluorescent-lit N_2-filled drybox. Variable-temperature ^1H NMR spectroscopic data of L_2TiMe_2 shows a singlet for the $-SiMe_3$ groups at temperatures down to −80 °C, indicative of rapid rotation of the amidinate ligands at an uncongested metal center. The methyl ligands are observed as a singlet at 1.96 ppm, which is significantly downfield of the related parameter of Cp_2TiMe_2 (−0.17 ppm).[41] Comparable Sc and Zr compounds[38,42,43] also display this trend, which can be attributed to relatively electron-deficient metal centers (L_2TiMe_2 is formally a 12-electron complex).

The Ti−C bonds of L_2TiMe_2 were found to be reactive toward a variety of protic reagents (water, alcohols, amines) in C_6D_6. Refluxing 1 equiv of *tert*-butylamine with the dimethyl in benzene followed by crystallization from hexanes yielded red-orange crystals of $L_2TiNCMe_3$ in 44% yield (Scheme 1). ^1H NMR spectroscopic data indicated a ratio of two amidinate ligands per *tert*-butyl group, and crystal structure analysis revealed the five-coordinate terminal imido functionality.[44] An ORTEP view of the molecular structure is shown in Figure 1, and bond lengths and angles are given in Table 1. The chelating amidinate ligands are bound to Ti with statistically identical Ti−N (average 2.151 Å) bond lengths. The imido functionality displays a short (1.656(9) Å) Ti−N bond comparable to reported values for $(TMEDA)TiCl_2NPh$ (1.702 Å),[45] $[(TMEDA)TiCl_2NC(Me)]_2$ (1.699(4) Å),[45] $Cp^*TiCl(Py)NBu^t$ (1.698(4) Å),[46] and $Ti(\eta^4\text{-}Me_8taa)(NBu^t)$ (1.724(4) Å) (taa = tetraaza[14]annulene).[47] The *tert*-butyl group is disordered over two positions (see Experimental Section for details)

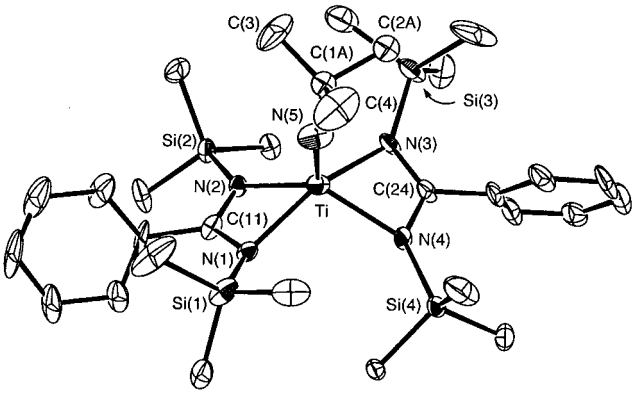

Figure 1. ORTEP view of $L_2TiNCMe_3$ drawn with 30% thermal ellipsoids. Atoms C(1B) and C(2B) of the disordered *tert*-butyl group are omitted for clarity.

Table 1. Selected Bond Distances (Å) and Angles (deg) for $L_2TiNCMe_3$

Ti−N(1)	2.152(7)	Ti−N(2)	2.147(7)
Ti−N(3)	2.156(8)	Ti−N(4)	2.148(8)
Ti−N(5)	1.656(9)	N(5)−C(1A)	1.46(2)
N(1)−Ti−N(2)	64.4(3)	N(1)−Ti−N(3)	155.3(3)
N(1)−Ti−N(4)	105.4(3)	N(1)−Ti−N(5)	101.3(4)
N(2)−Ti−N(3)	103.5(3)	N(2)−Ti−N(4)	64.0(3)
N(2)−Ti−N(5)	114.2(4)	N(3)−Ti−N(4)	64.0(3)
N(3)−Ti−N(5)	103.4(4)	N(4)−Ti−N(5)	114.2(4)
Ti−N(5)−C(1A)	166(1)		

giving somewhat unreliable bond lengths and angles for the imido ligand. What is certain is that the imido ligand is bent, with a Ti−N−C angle of 166(1)°. This suggests that the shortness of the bond is possibly due to low steric crowding instead of a true Ti−N triple bond.

Compared to related zirconocene imido derivatives,[48] the Ti−imido linkage appears to be relatively inert. In C_6D_6 solutions, no reaction was observed with ditolylacetylene or H_2 (2 atm) at 50 °C overnight. Reactivity was observed, however, between $L_2TiNCMe_3$ and acetone in C_6D_6 (eq 1). Complete conversion to $L_2Ti(\mu\text{-}O)_2TiL[\eta^1\text{-}NC(Ph)N(SiMe_3)_2]$ occurred within 2 h. The dititanium bis(μ-oxo) product was independently prepared by reaction of $(L_2Ti)_2(\mu\text{-}N_2)$ with O_2 (see later).

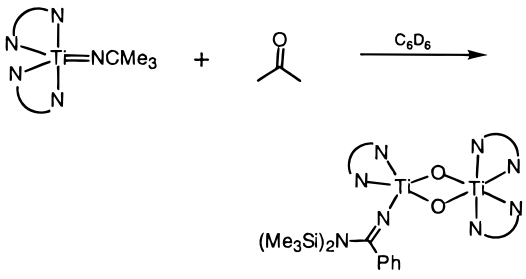

(1)

Reduction Chemistry of L_2TiCl_2. As shown in Scheme 2, the 1% Na/Hg amalgam reduction of L_2TiCl_2 in THF proceeded smoothly overnight giving paramagnetic $L_2TiCl(THF)$, which was isolated as green crystals from hexanes. Isolated yields were low (<30%) due to the high solubility of the product and the floculent nature of the crystalline solid. Solid-state magnetic-susceptibility measurements ($\mu_{eff} = 1.6\ \mu_B$) are consis-

(41) Samuel, E.; Rausch, M. D. *J. Am. Chem. Soc.* **1973**, *95*, 6263.
(42) Hagadorn, J. R.; Arnold, J. *Organometallics* **1996**, *15*, 984.
(43) Hagadorn, J. R.; Arnold, J. *J. Chem. Soc., Dalton Trans.* **1997**, 3087.
(44) Mountford, P. *Chem. Commun.* **1997**, 2127.
(45) Duchateau, R.; Williams, A. J.; Gambarotta, S.; Chiang, M. Y. *Inorg. Chem.* **1991**, *30*, 4863.
(46) Bai, Y.; Noltemeyer, M.; Roesky, H. W. *Z. Naturforsch.* **1991**, *46b*, 1357.
(47) Dunn, S. C.; Bastanov, A. S.; Mountford, P. *J. Chem. Soc., Chem. Commun.* **1994**, 2007.
(48) Walsh, P. J.; Hollander, F. J.; Bergman, R. G. *J. Am. Chem. Soc.* **1988**, *110*, 8729.

Scheme 2

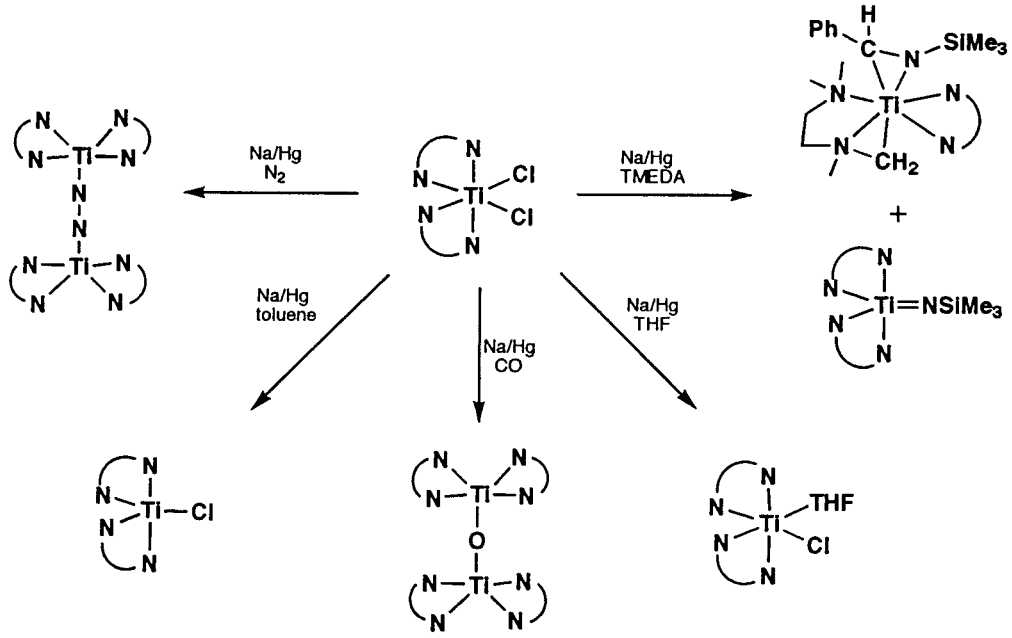

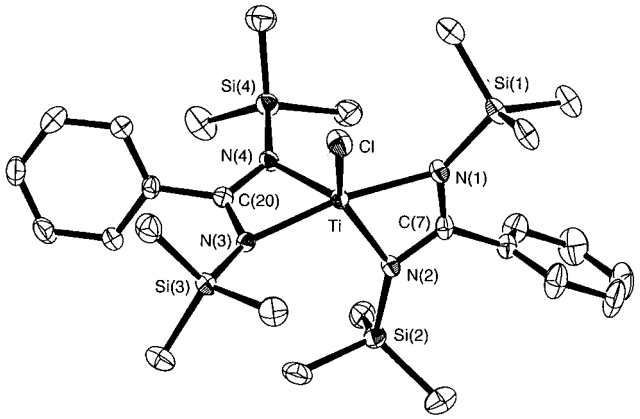

Figure 2. ORTEP view of L_2TiCl drawn with 50% thermal ellipsoids.

tent with a Ti(III) metal center. Recrystallization from hexanes resulted in the growth of red crystals intermixed with $L_2TiCl(THF)$. This proved to be the related base-free chloride, which was conveniently prepared by the 1% Na/Hg reduction of L_2TiCl_2 in toluene. Following hexanes workup, paramagnetic crystals of L_2TiCl were isolated in 57% yield. Although excess Na is used in the overnight reaction, further reduction to Ti(II) appears to be slow under these conditions (see later). Combustion analysis and magnetic-susceptibility measurements (μ_{eff} = 1.6 μ_B) are consistent with the expected base-free product. X-ray crystallography revealed the base-free chloride to be monomeric with five-coordinate titanium. An ORTEP view is shown in Figure 2, with bond angles and lengths given in Table 2. The structure can be contrasted with that of the related titanocene derivative $(Cp_2TiCl)_2$, which is dimeric with bridging chloride ligands (average Ti−Cl, 2.543 Å).[49] As expected, the Ti−Cl bond (2.328(1) Å) is slightly longer than the related parameter of the Ti(IV) dichloride L_2TiCl_2 (2.257(3) Å).[24] The Ti−N bonds show a

Table 2. Selected Bond Distances (Å) and Angles (deg) for L_2TiCl

Ti−Cl	2.328(1)	Ti−N(1)	2.164(3)
Ti−N(2)	2.071(3)	Ti−N(3)	2.119(3)
Ti−N(4)	2.051(3)	Si(1)−N(1)	1.749(3)
Si(2)−N(2)	1.749(3)	Si(3)−N(3)	1.756(3)
Si(4)−N(4)	1.745(3)	N(1)−C(7)	1.315(4)
N(2)−C(7)	1.352(4)	N(3)−C(20)	1.328(4)
N(4)−C(20)	1.347(4)		
Cl−Ti−N(1)	94.68(8)	Cl−Ti−N(2)	144.45(9)
Cl−Ti−N(3)	95.77(8)	Cl−Ti−N(4)	110.25(9)
N(1)−Ti−N(2)	64.3(1)	N(1)−Ti−N(3)	168.5(1)
N(1)−Ti−N(4)	115.0(1)	N(2)−Ti−N(3)	104.2(1)
N(2)−Ti−N(4)	104.8(1)	N(3)−Ti−N(4)	65.5(1)
Ti−N(1)−Si(1)	137.2(2)	Ti−N(2)−Si(2)	138.5(2)
Ti−N(3)−Si(3)	134.4(2)	Ti−N(4)−Si(4)	134.7(2)

slight elongation for Ti−N(1) and Ti−N(3) due to their positions trans to each other. Other metrical values associated with the benzamidinate ligands are unremarkable.

Unlike the related Lewis-base-containing compound $L_2Ti(\mu\text{-}Cl)_2Li(TMEDA)$,[34] L_2TiCl appears to be a good starting material for the preparation of Ti(III) alkyls by salt-metathesis methodology. Reaction of the chloride with $LiCH_2SiMe_3$ in toluene (eq 2) gave a dark red solution, which upon hexanes workup and crystallization from HMDSO yielded the Ti(III) alkyl $L_2TiCH_2SiMe_3$ in 64% yield. The related methyl derivative was

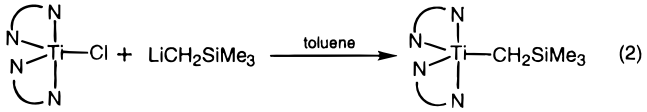

(2)

prepared by the 1% Na/Hg reduction of $L_2Ti(Me)Cl$ in THF (eq 3). Removal of the volatile materials affords a

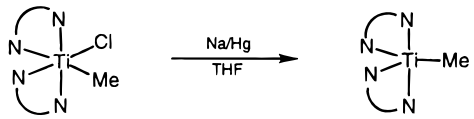

(3)

paramagnetic red solid that appears (by ^1H NMR) to

(49) Jungst, R.; Sekutowski, D.; Davis, J.; Luly, M.; Stucky, G. *Inorg. Chem.* **1977**, *16*, 1645.

contain coordinated THF, but the base can be easily removed by prolonged evacuation or successive addition/evaporation of toluene to the solid followed by crystallization from HMDSO. X-ray crystallographic data[39] of the methyl derivative revealed a monomeric five-coordinate titanium with an apparent agostic interaction between Ti and one of the methyl C−H bonds (Ti−H, 2.51(5) Å; Ti−C−H, 104(3)°).

Further reduction of L_2TiCl_2 with 1% Na/Hg to a Ti(II) species occurs over 2−3 days in toluene. When the reaction was carried out under N_2, this was observed as a change in color from red to blue-black. After 3 days of stirring, ^{1}H NMR spectroscopic analysis of the crude solution revealed the absence of any starting material or L_2TiCl and the presence of a single diamagnetic product. After removal of volatile materials, extraction into hexanes, and cooling to −40 °C, blue-black crystals of the dinitrogen complex $(L_2Ti)_2(\mu\text{-}N_2)$ were isolated in moderate yield (41% from 3 crops). The X-ray crystal structure[39] revealed five-coordinate titanium and the end-on bonding mode of the bridging N_2. The compound is thermally robust and failed to react with H_2 (6 atm), CO (2 atm), ethylene (1atm), PMe_3, or ditolylacetylene in C_6D_6, even after heating to 70 °C for several days.

Carrying out the 1% Na/Hg reduction of L_2TiCl_2 in toluene under an atmosphere of CO gave a red-black solution after 2 days. Hexanes workup of the solution and cooling to −40 °C gave low yields of paramagnetic, dark red crystals. Instead of the anticipated Ti(II) dicarbonyl, the compound was determined by crystallography to be $(L_2Ti)_2(\mu\text{-}O)$.[39] Since carrying out the reaction in the absence of CO (under argon) failed to give this product, we felt it likely that the oxo ligand was formed by the cleavage of CO. Additionally, it was found to be highly reactive with O_2, apparently yielding multiple diamagnetic products in C_6D_6. To confirm the CO bond cleavage, we carried out the reduction under an atmosphere of $C^{18}O$ (eq 4). Electron-impact mass

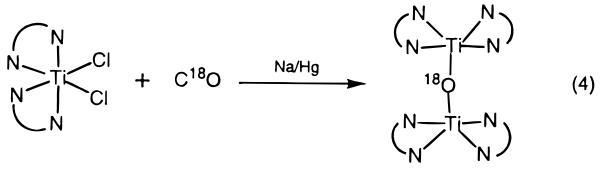

(4)

spectroscopy of this product confirmed CO as the sole oxygen source for the μ-oxo ligand. Due to the low isolated yields of the μ-oxo derivative, we presume that additional products are formed during this reaction, but to date we have been unable to isolate them and the fate of the carbon atom remains to be determined. Related reactions involving low-valent tantalum are known to form oxo and dicarbide species,[50] nonetheless, in general, CO cleavage remains relatively rare.[51] The compound is paramagnetic (μ_{eff} = 2.4 μ_B) with a magnetic moment that is consistent with two essentially uncoupled d^1-Ti centers. This value is similar to those for $(Me_3tacn)_2Ti_2(NCO)_4(\mu\text{-}O)$ and $(Me_3tacn)_2Ti_2(NCS)_4(\mu\text{-}O)$ (Me_3tacn = 1,4,7-trimethyl-1,4,7-triazacyclononane) which display only weakly antiferromagnetic coupling (J = 7 cm^{-1} average).[52]

Use of the chelating diamine TMEDA in an additional attempt to trap the Ti(II) intermediate led to unprecedented reactivity and the formation of two products. The 1% Na/Hg reduction of L_2TiCl_2 in the presence of excess TMEDA in toluene occurred overnight, giving a dark purple-brown solution. Following hexanes workup and cooling to −40 °C, yellow crystals of $L_2TiNSiMe_3$ were isolated in 24% yield (Scheme 2). Characterization by ^{1}H NMR spectroscopy reveals two sharp singlets in the $-SiMe_3$ region with relative intensities of 36:9, and its $^{13}C\{^1H\}$ NMR spectrum is very similar to that of $L_2TiNCMe_3$. Additionally, combustion analysis and EI-MS data support its formulation. Further concentration of the mother liquor and cooling yielded red-black crystals of a second product $LTi[\eta^2\text{-}Me_3SiNC(H)Ph][\eta^3\text{-}CH_2N(Me)CH_2CH_2N(Me)_2]$ in 42% yield. The solid-state structure of the product was determined by X-ray crystallography, revealing a seven-coordinate Ti bonded to an amidinate ligand, an η^2-imine, and a tridentate cyclometalated TMEDA ligand.[39] The long C−N(imine) bond (1.446(8) Å) implies substantial metallaaziridine character and formulation of the product as Ti(IV) as opposed to Ti(II). The room-temperature ^{1}H NMR spectrum is complex, showing a multitude of broad resonances, apparently due to hindered rotation and/or the presence of diastereomers. On warming to 90 °C, however, the spectrum sharpens to give a pattern consistent with the solid-state structure, with three singlets for the inequivalent $-SiMe_3$ groups and a singlet for the imine hydrogen at 5.49 ppm. The complexity of the room-temperature spectrum is independent of concentration or the addition of TMEDA, consistent with an intramolecular rearrangement.

Lewis-Base Adducts of $(L_2Ti)_2(\mu\text{-}N_2)$. As stated above, the bridging-dinitrogen complex $(L_2Ti)_2(\mu\text{-}N_2)$ was found to be unreactive toward a variety of σ-donor and π-acceptor ligands. It was observed, however, that the addition of a large excess of THF to a toluene solution of the compound changed the color from dark blue to green. Attempts to isolate a THF-containing product by crystallization from THF/hexanes were unsuccessful, and removal of the volatile materials afforded pure starting material. By analogy to other Lewis-base adducts mentioned below, we believe the green THF-containing product to be $[L_2Ti(THF)]_2(\mu\text{-}N_2)$ (eq 5). In

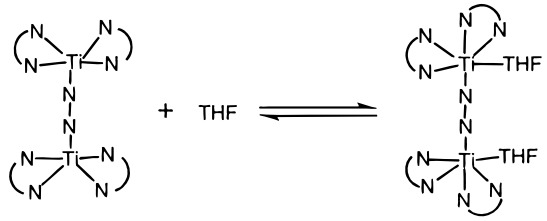

(5)

contrast, addition of pyridine immediately gave a red solution, which retained its color upon removal of volatile materials under reduced pressure. Extraction of the residue into hexanes and cooling to −30 °C yielded dark red diamagnetic crystals in moderate yield. ^{1}H

(50) LaPointe, R. E.; Wolczanski, P. T.; Mitchell, J. F. *J. Am. Chem. Soc.* **1986**, *108*, 6382.

(51) For examples, see: Planalp, R. P.; Andersen, R. A.; Zalkin, A. *Organometallics* **1983**, *2*, 16. Chisholm, M. H.; Hammond, C. E.; Johnston, V. J.; Streib, W. E.; Huffman, J. C. *J. Am. Chem. Soc.* **1992**, *114*, 7056. Arnold, J.; Tilley, T. D.; Rheingold, A. L.; Geib, S. J.; Arif, A. M. *J. Am. Chem. Soc.* **1989**, *111*, 149−164 and references therein.

(52) Jeske, P.; Wiegardt, K.; Nuber, B. *Inorg. Chem.* **1994**, *33*, 47.

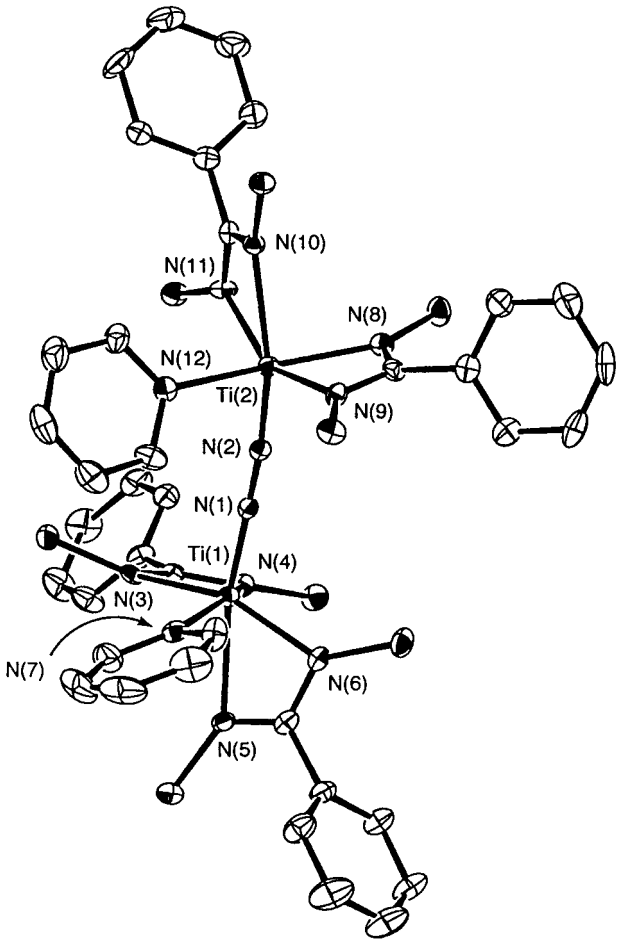

Figure 3. ORTEP view of $[L_2Ti(Py)]_2(\mu\text{-}N_2)$ drawn with 50% thermal ellipsoids. Methyl groups are omitted for clarity.

NMR data showed a pyridine-to-amidinate ratio of 1:2, and IR spectroscopy revealed a stretch at 1602 cm^{-1} which is characteristic of coordinated Py. X-ray crystallography confirmed the product to be $[L_2Ti(Py)]_2(\mu\text{-}N_2)$ (eq 6), with an intact Ti_2N_2 core. An ORTEP view is

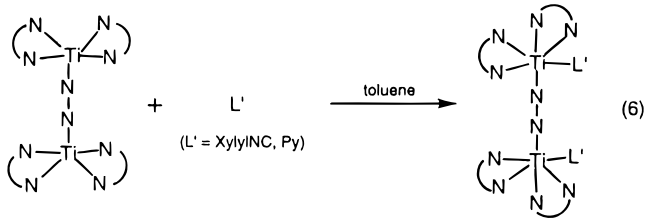

(6)

shown in Figure 3, with bond distances and angles given in Table 3. Shown in Figure 4 are a few other structurally characterized complexes containing the $Ti_2(\mu\text{-}N_2)$ core. Compared to the five-coordinate Ti centers of $(L_2Ti)_2(\mu\text{-}N_2)$, the metal centers of the Py adduct are much more crowded. This is reflected in increased Ti−N bond lengths to the μ-N_2 ligand (Ti(1)−N(1), 1.799(4) Å; Ti(2)−N(2), 1.798(4) Å). The μ-N_2 ligand is highly reduced in the diamagnetic complex, with a long N(1)−N(2) bond of 1.264(5) Å that is slightly shorter than that of $(L_2Ti)_2(\mu\text{-}N_2)$ (1.275(6) Å) and $\{[(Me_3Si)_2N]Ti(TMEDA)Cl\}_2(\mu\text{-}N_2)$[53] (1.289(9) Å) but much longer than that of the related metallocene derivative $(Cp^*_2Ti)_2(\mu\text{-}N_2)$[54] (1.165(14), 1.155(14) Å). This extreme reduction of the N_2-ligand correlates well with its relative nonlability compared to metallocene derivatives $(Cp^*_2Ti)_2(\mu\text{-}N_2)$[55] and $[Cp_2Ti(PMe_3)]_2(\mu\text{-}N_2)$,[56] which lose N_2 at room temperature. Analogous to the formation of the pyridine adduct, addition of 2 equiv of XylylNC to $(L_2Ti)_2(\mu\text{-}N_2)$ in toluene afforded the diamagnetic isocyanide adduct $[L_2Ti(CNXylyl)]_2(\mu\text{-}N_2)$, which was isolated as a rose-colored floculent solid (50% yield) following hexanes workup. Interestingly, the IR spectrum of this complex shows a blue-shifted ν_{CN} at 2143 cm^{-1} compared to that of free XylylNC (2115 cm^{-1}). These data together with the robust nature of the $Ti_2(\mu\text{-}N_2)$ core suggests substantial Ti(IV) character for the dinitrogen complexes.

Table 3. Selected Bond Distances (Å) and Angles (deg) for $[L_2Ti(Py)]_2(\mu\text{-}N_2)$

Ti(1)−N(1)	1.799(4)	Ti(1)−N(3)	2.207(4)
Ti(1)−N(4)	2.185(4)	Ti(1)−N(5)	2.337(4)
Ti(1)−N(6)	2.111(4)	Ti(1)−N(7)	2.254(4)
Ti(2)−N(2)	1.798(4)	Ti(2)−N(8)	2.156(4)
Ti(2)−N(9)	2.251(4)	Ti(2)−N(10)	2.371(4)
Ti(2)−N(11)	2.129(4)	Ti(2)−N(12)	2.233(4)
N(1)−N(2)	1.264(5)		
N(1)−Ti(1)−N(3)	101.8(2)	N(1)−Ti(1)−N(4)	105.4(2)
N(1)−Ti(1)−N(5)	161.2(2)	N(1)−Ti(1)−N(6)	103.6(2)
N(1)−Ti(1)−N(7)	91.7(2)	N(3)−Ti(1)−N(4)	62.7(1)
N(3)−Ti(1)−N(5)	95.3(1)	N(3)−Ti(1)−N(6)	153.1(2)
N(3)−Ti(1)−N(7)	98.9(2)	N(4)−Ti(1)−N(5)	89.4(1)
N(4)−Ti(1)−N(6)	101.8(1)	N(4)−Ti(1)−N(7)	77.8(1)
N(5)−Ti(1)−N(6)	61.1(2)	N(6)−Ti(1)−N(7)	89.0(1)
N(2)−Ti(2)−N(8)	102.7(2)	N(2)−Ti(2)−N(9)	104.0(2)
N(2)−Ti(2)−N(10)	162.7(2)	N(2)−Ti(2)−N(11)	103.1(2)
N(2)−Ti(2)−N(12)	90.3(2)	N(8)−Ti(2)−N(9)	62.0(1)
N(8)−Ti(2)−N(10)	87.0(1)	N(8)−Ti(2)−N(11)	103.2(2)
N(8)−Ti(2)−N(12)	154.5(1)	N(9)−Ti(2)−N(10)	93.2(1)
N(9)−Ti(2)−N(11)	151.4(2)	N(9)−Ti(2)−N(12)	93.8(1)
N(10)−Ti(2)−N(11)	60.3(1)	N(10)−Ti(2)−N(11)	60.3(1)
N(10)−Ti(2)−N(12)	86.5(1)	N(11)−Ti(2)−N(12)	94.9(2)
Ti(1)−N(1)−N(2)	173.0(3)	Ti(2)−N(2)−N(1)	174.4(3)

Oxidation Reactions of $(L_2Ti)_2(\mu\text{-}N_2)$. Several low-valent group 4 metallocene derivatives have been successfully used as precursors for the syntheses of complexes containing metal−(group 16) bonds. Specific examples include the oxidation of $Cp^*_2Zr(CO)_2$ by elemental sulfur in the presence of pyridine yielding the Zr(IV) sulfido $Cp^*_2Zr(S)Py$[57] and the formation of $Cp^*_2Ti(O)Py$ from reaction of $Cp^*_2Ti(C_2H_4)$ with N_2O in THF/pyridine.[58] In exploring similar reactivity with $(L_2Ti)_2(\mu\text{-}N_2)$, we found that it was readily oxidized by a variety of oxygen and sulfur sources. The dinitrogen complex reacted with dry oxygen in hexanes/pyridine (20:1), immediately forming a clear orange solution. Removal of volatile materials under reduced pressure afforded an orange solid, which displayed NMR spectroscopic and analytical data consistent with its formulation as the peroxo derivative $L_2Ti(\eta^2\text{-}O_2)Py$ (Scheme 3). Due to multiple bands in the region, we were unable to assign the ν_{O-O} stretch in the infrared spectrum, however, the seven-coordinate structure was confirmed by X-ray crystallography.[40]

(53) Duchateau, R.; Gambarotta, S.; Beydoun, N.; Bensimon, C. *J. Am. Chem. Soc.* **1991**, *113*, 8986.

(54) Sanner, R. D.; Duggan, D. M.; McKenzie, T. C.; Marsh, R. E.; Bercaw, J. E. *J. Am. Chem. Soc.* **1976**, *98*, 8358.

(55) Bercaw, J. E. *J. Am. Chem. Soc.* **1974**, *96*, 5087.

(56) Berry, D. H.; Procopio, L. J.; Carroll, P. J. *Organometallics* **1988**, *7*, 570.

(57) Howard, W. A.; Parkin, G. *Organometallics* **1993**, *12*, 2363.

(58) Smith, M. R.; Matsunaga, P. T.; Andersen, R. A. *J. Am. Chem. Soc.* **1993**, *115*, 7049.

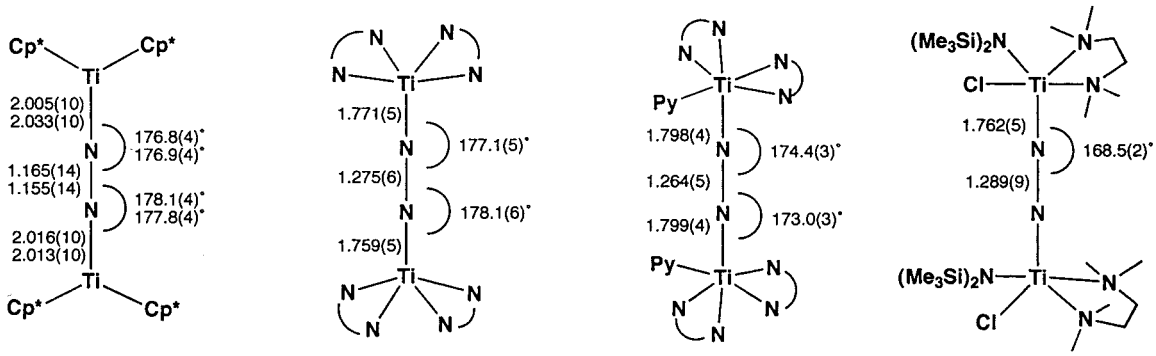

Figure 4. Comparison of the core structures of a few $Ti_2(\mu\text{-}N_2)$ complexes. See refs 39, 52, 53.

Scheme 3

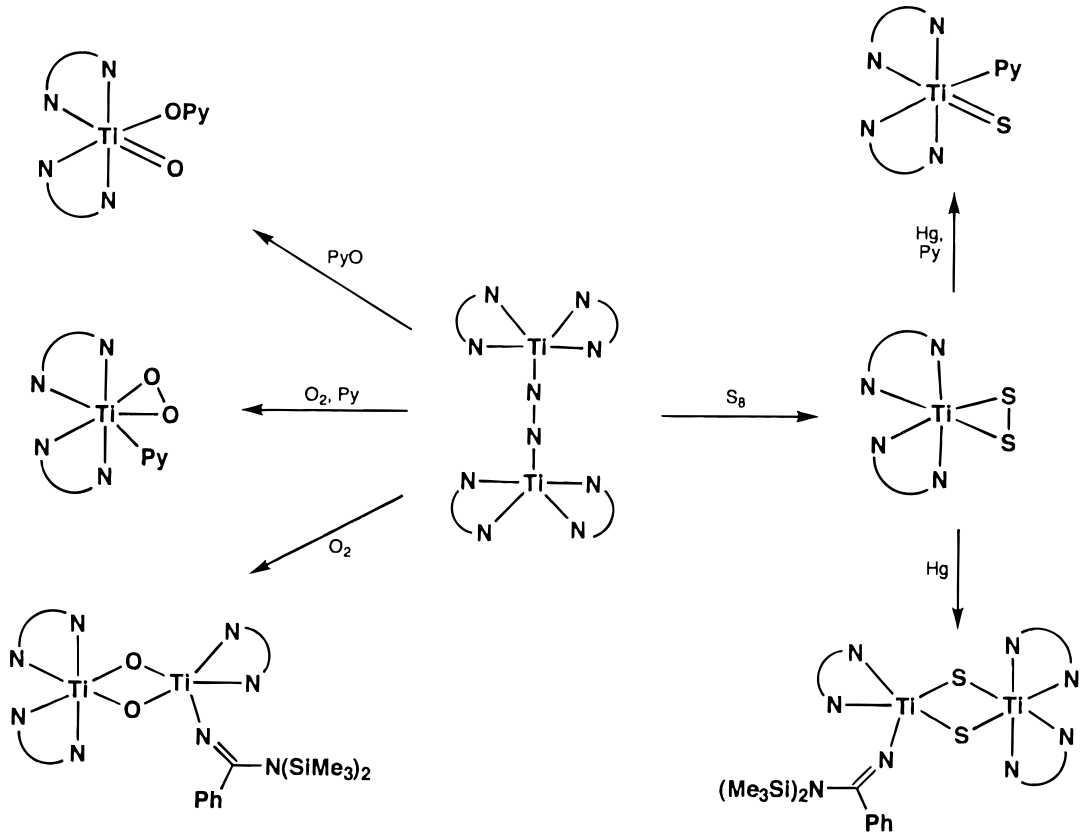

When the above reaction was repeated in the absence of pyridine (in C_6D_6), a yellow-orange solution formed immediately that displayed a complex ^{1}H NMR spectrum with at least eight partially overlapping peaks in the $-SiMe_3$ region. Use of excess N_2O in place of oxygen, likewise, formed the same product. The reaction was found to proceed cleanest, however, when carried out with oxygen (1 atm) on powdered $(L_2Ti)_2(\mu\text{-}N_2)$. After exposure to oxygen for a few minutes a bright yellow solid formed, which displayed spectroscopic data (IR, NMR) identical to that of the product observed in the solution reactions. Combustion data was consistent with the empirical formula $(L_2TiO)_n$, and the solid-state structure was determined to explain the nature of the complex spectroscopic data. This revealed the product to be $L_2Ti(\mu\text{-}O)_2TiL[\eta^1\text{-}NC(Ph)N(SiMe_3)_2]$, which contains an η^1-iminoamine ligand formed by an unusual silyl group migration at an amidinate ligand. The bridging-oxo complex failed to react with several equivalents of pyridine and is stable at 100 °C in toluene-d_8. At that temperature, ^{1}H NMR spectroscopy revealed only three signals in the $-SiMe_3$ region, which is consistent with the solid-state structure (assuming fast ligand rotation).

Reaction of $(L_2Ti)_2(\mu\text{-}N_2)$ with an excess of pyridine *N*-oxide in toluene/pyridine (20:1) gave a lavender solution after stirring overnight. Upon workup in Et_2O and cooling to −30 °C, crystals of the terminal oxo L_2-Ti(O)OPy were isolated in moderate yield. At 75 °C in C_6D_6, the complex undergoes partial decomposition to $L_2Ti(\mu\text{-}O)_2TiL[\eta^1\text{-}NC(Ph)N(SiMe_3)_2]$ overnight, but the reaction appears to be hindered by the Py−O released. The structure of the complex was determined by X-ray crystallography, and an ORTEP view is shown in Figure 5, with bond lengths and angles displayed in Table 4. The complex features a pseudo-octahedral metal center. The Ti−oxo bond (1.654(2) Å) is comparable to related parameters of $Cp^*_2Ti(O)$(4-phenylpyridine) (1.665(3) Å),[58] (OEP)TiO (1.613(5) Å) (OEP = octaethylporphyrin),[59] and (2,6-^{i}Pr$_2$-C_6H_4O)Ti(O)$(NC_5H_4\text{-}4\text{-}NC_4H_8)_2$ (1.657-

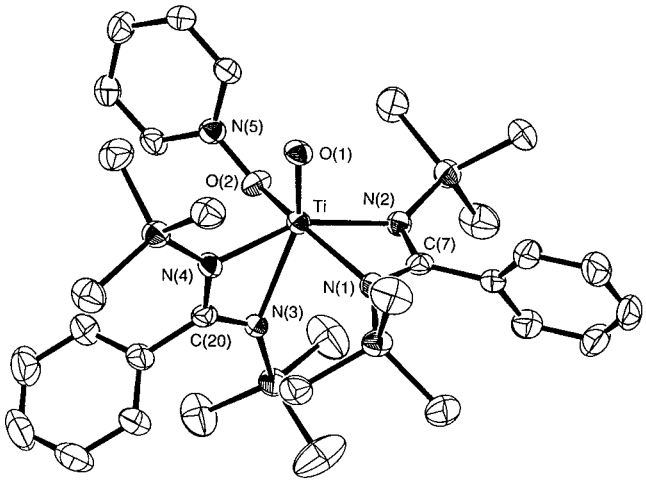

Figure 5. ORTEP view of $L_2Ti(O)OPy$ drawn with 50% thermal ellipsoids.

Table 4. Selected Bond Distances (Å) and Angles (deg) for $L_2Ti(O)OPy$

Ti−O(1)	1.654(2)	Ti−O(2)	2.036(2)
Ti−N(1)	2.153(2)	Ti−N(2)	2.173(3)
Ti−N(3)	2.394(3)	Ti−N(4)	2.081(3)
O(2)−N(5)	1.348(3)	N(1)−C(7)	1.331(4)
N(2)−C(7)	1.335(4)	N(3)−C(20)	1.309(4)
N(4)−C(20)	1.352(4)		
O(1)−Ti−O(2)	98.5(1)	O(1)−Ti−N(1)	103.1(1)
O(1)−Ti−N(2)	103.7(1)	O(1)−Ti−N(3)	157.3(1)
O(1)−Ti−N(4)	97.4(1)	O(2)−Ti−N(1)	151.05(9)
O(2)−Ti−N(2)	93.39(9)	O(2)−Ti−N(3)	80.54(9)
O(2)−Ti−N(4)	95.45(9)	N(1)−Ti−N(2)	63.1(1)
N(1)−Ti−N(3)	86.57(9)	N(1)−Ti−N(4)	100.5(1)
N(2)−Ti−N(3)	99.02(9)	N(2)−Ti−N(4)	155.7(1)
N(3)−Ti−N(4)	60.36(9)	Ti−O(2)−N(5)	125.5(2)

(6) Å).[60] The elongated Ti−N(3) bond length (2.394(3) Å) compared to the other Ti−N bonds (average 2.136 Å) is attributed to the strong trans influence of the oxo ligand. Comparison to the related sulfido derivative $L_2Ti(S)Py$ reveals very similar metrical trends but a less pronounced trans influence (Figure 8). The amidinate ligands are bonded in the typical bidentate manner with the titanium sitting essentially in the NCN planes.

Excess sulfur was found to react with $(L_2Ti)_2(\mu\text{-}N_2)$ in toluene giving a teal solution within 1 h. The volatile materials were stripped off, and the residue was crystallized from hexanes yielding the persulfido derivative $L_2Ti(\eta^2\text{-}S_2)$ in good yield. ^1H NMR spectroscopic data shows a sharp singlet for the $-SiMe_3$ groups indicative of a sterically uncongested metal center. The solid-state structure was determined by X-ray crystallography. Each asymmetric unit contains two independent molecules shown as ORTEP views in Figure 6, with bonds and angles given in Table 5. The two molecules each feature pseudo-octahedral titanium with nearly identical conformations. Titanium−sulfur bonds vary only slightly in length, ranging from 2.308(2) to 2.317(2) Å. The S−S bonds are statistically identical with values of 2.074(2) and 2.075(2) Å. As shown in Figure 8, the S−Ti−S angles (average 53.3°) are larger that the related parameter of $L_2Ti(\eta^2\text{-}O_2)Py$ (O−Ti−O, 46.6°), reflecting the size of the persulfido ligand. This is likely responsible for the lack of reactivity that $L_2Ti(\eta^2\text{-}S_2)$ displays toward pyridine.

The persulfido complex was found to react slowly with metallic mercury in toluene. After the mixture was stirred vigorously for 17 h, the initially teal solution became red with a good amount of insoluble gray precipitate, presumably HgS. Filtration and removal of the volatile materials under reduced pressure afforded an orange solid that displayed a complex ^1H NMR spectrum similar to that described for $L_2Ti(\mu\text{-}O)_2TiL[\eta^1\text{-}NC(Ph)N(SiMe_3)_2]$, so it seemed likely that we had prepared the sulfur-containing analogue. Additionally, IR spectroscopic data revealed a strong absorbance at 1518 cm^{-1}, which we assign as $\nu_{C=N}$ of the η^1-NC(Ph)N$(SiMe_3)_2$ ligand. Crystallization of the solid from Et_2O gave crystals that analyzed for the formula $(L_2TiS)_n$, and the X-ray structure confirmed that the complex was indeed $L_2Ti(\mu\text{-}S)_2TiL[\eta^1\text{-}NC(Ph)N(SiMe_3)_2]$. An ORTEP diagram is shown in Figure 7, with metrical parameters given in Table 6. Structurally, the complex is very similar to the bridging-oxo analogue (Figure 8) with a planar Ti_2S_2 core (torsion angle Ti(1)−S(1)−Ti(2)−S(2) = 1.06(5)°) and alternating Ti−S bond lengths. The Ti−S−Ti angles (average 89.7°) are relatively acute, yet the Ti−Ti distance of 3.27 Å is considerably longer than in the oxo derivative (2.75 Å). The η^1-iminoamine ligand, bound to the five-coordinate Ti, is bent with a Ti−N−C angle of 158.0(3)° and a short Ti−N bond of 1.831(4) Å. The shortness of the bond suggests multiple bond character,[61] as a pure single bond is expected to be about 1.96 Å. Additionally, the disilylamine group appears to favor being coplanar with the N(7)−C(46) double bond (torsion angles Si(7)−N(8)−C(46)−N(7), 19.0(5)°; Si(8)−N(8)−C(46)−N(7), 26.1(3)°), possibly resulting in a delocalized Ti−N−C−N system.

As shown in Scheme 3, the reaction of $L_2Ti(\eta^2\text{-}S_2)$ with mercury in the presence of pyridine allowed for the trapping of the terminal sulfido derivative $L_2Ti(S)Py$. Following hexanes workup, the product was isolated as orange-red crystals from Et_2O/hexanes in 23% yield. Infrared spectroscopy showed an absorbance at 1601 cm^{-1}, which is characteristic of coordinated pyridine, and ^1H NMR spectroscopic data (in C_6D_6) confirmed an amidinate-to-pyridine ratio of 2:1. When several equivalents of the base were added to a $L_2Ti(S)Py$ solution, a single broadened signal was observed for the *ortho*-pyridine protons, revealing rapid exchange. Heating a C_6D_6 solution of the sulfido to 85 °C for 1 h resulted in ca. 50% conversion to $L_2Ti(\mu\text{-}S)_2TiL[\eta^1\text{-}NC(Ph)N(SiMe_3)_2]$. Heating for an additional 12 h resulted in almost no change, possibly due to the presence of free pyridine in solution inhibiting further reaction. A dissociative mechanism was supported by attempting the same thermolysis in the presence of 9 equiv of free pyridine, which resulted in almost no loss of the terminal sulfido after heating for 1 h.

Summary and Conclusions

We have shown that the BTBA ligand is capable of supporting a wide range of unusual titanium chemistry

(59) Guilard, R.; Latour, J.-M.; Lecomte, C.; Marchon, J.-C.; Protas, J.; Ripoll, D. *Inorg. Chem.* **1978**, *17*, 1228.
(60) Hill, J. E.; Fanwick, P. E.; Rothwell, I. P. *Inorg. Chem.* **1989**, *28*, 3602.
(61) Giolando, D. M.; Kirschbaum, K.; Graves, L. J.; Bolle, U. *Inorg. Chem.* **1992**, *31*, 3887.

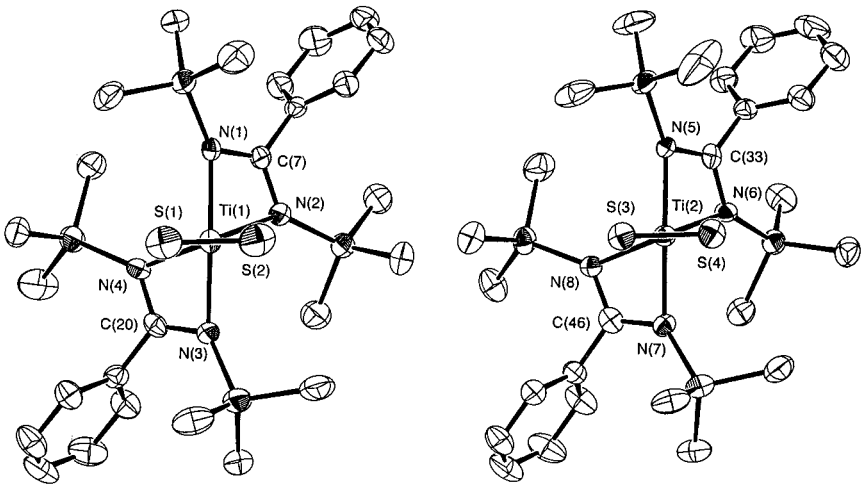

Figure 6. ORTEP view of two independent molecules of $L_2Ti(\eta^2\text{-}S_2)$ drawn with 50% thermal ellipsoids.

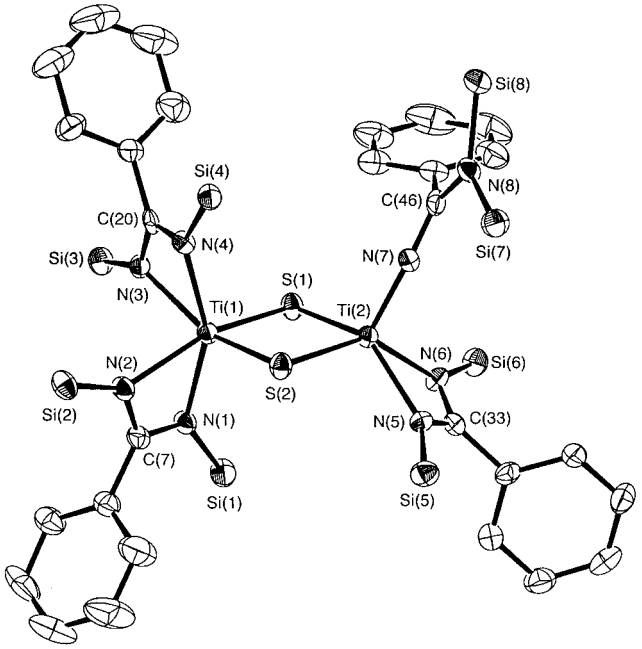

Figure 7. ORTEP view of $L_2Ti(\mu\text{-}S)_2TiL[\eta^1\text{-}NC(Ph)N(SiMe_3)_2]$ drawn with 50% thermal ellipsoids. Methyl groups are omitted for clarity.

in a variety of oxidation states. In several instances, the L_2Ti compounds show reactivity comparable to that seen in related Cp_2Ti derivatives but with some notable differences; most of these may be attributed to the less electron-rich nature of the BTBA series of compounds relative to Cp systems. The unusual 1,3-silyl migration chemistry to form $\eta^1\text{-}NC(Ph)N(SiMe_3)_2$ species and the C−N bond cleavage reactions to form imido complexes reinforces the notion, well-documented in Cp chemistry, that examples of completely "innocent" spectator ligands are rare. Further reactivity studies of new complexes will be presented in future publications.

Experimental Section

General Considerations. Standard Schlenk-line and glovebox techniques were used. Tetrahydrofuran (THF), diethyl ether, and hexanes were distilled from sodium/benzophenone under nitrogen. Dichloromethane and *tert*-butylamine were distilled from CaH_2 under nitrogen. C_6D_6 was vacuum transferred from sodium/benzophenone. Hexamethyldisiloxane (HMDSO), *N*,*N*,*N*′,*N*′-tetramethylethylenediamine (TMEDA), and pyridine (Py) were distilled from Na under argon. Carbon monoxide was used directly from cylinders without purification. 2,6-Dimethylphenyl isocyanide (XylylNC) was purchased from Fluka and used as received. Elemental sulfur and pyridine *N*-oxide (PyO) were purchased from Aldrich and used as received. Oxygen was passed through a column of Drierite prior to use. The compounds L_2TiCl_2,[24,34] $LiCH_2SiMe_3$,[62] and Me_2Mg[63,64] were prepared according to literature procedures. $PhCH_2MgCl$ was prepared by the addition of $PhCH_2Cl$ to a Mg suspension in Et_2O. Melting points were determined in sealed capillary tubes under nitrogen and are uncorrected. ^1H and $^{13}C\{^1H\}$ NMR spectra were recorded at ambient temperatures unless stated otherwise. Chemical shifts (δ) are given relative to residual protium in the deuterated solvent at δ 7.15 and 7.24 for C_6D_6 and $CDCl_3$, respectively. IR samples were prepared as mineral oil mulls and taken between KBr plates. Elemental analyses and mass spectral data were determined within the College of Chemistry, University of California, Berkeley. Magnetic moments were determined using a Johnson-Mathey MSB-1 balance unless stated otherwise. Single-crystal X-ray structure determinations were performed at CHEXRAY, University of California, Berkeley.

$L_2Ti(Me)Cl$. Benzene (125 mL) was added to a 250-mL round-bottomed flask containing L_2TiCl_2 (6.19 g, 9.58 mmol) forming a clear orange solution. At 0 °C, an ethereal solution of Me_2Mg (15.5 mL, 4.79 mmol) was added dropwise, forming a red solution. After addition, the mixture was stirred overnight at room temperature. The volatile materials were then removed under reduced pressure, and the red-pink solid was extracted with CH_2Cl_2 (125 mL). Filtration through a Celite pad on a fritted disk followed by concentration to 80 mL and cooling to −40 °C afforded dark red crystals of analytically pure product (4.3 g, 72%). Mp: 191−194 °C. ^1H NMR (C_6D_6, 300 MHz): δ 7.30−7.25 (m, 4H), 7.02−6.98 (m, 6H), 2.26 (s, 3H), 0.18 (s, 36H). $^{13}C\{^1H\}$ NMR (C_6D_6, 75.5 MHz): δ 183.0, 139.8, 129.2, 126.3, 74.7, 2.3. IR: 1418 (s), 1247 (m), 1164 (w), 1076 (w), 1032 (w), 996 (m), 973 (m), 922 (w), 841 (s, br), 790 (m), 761 (m), 739 (m), 702 (m), 509 (m) cm^{-1}. Anal. Calcd for $C_{27}H_{49}ClN_4Si_4Ti$: C, 51.85; H, 7.90; N, 8.96. Found: C, 51.73; H, 7.73; N, 8.94.

L_2TiMe_2. To a clear orange solution of L_2TiCl_2 (3.00 g, 4.65 mmol) in diethyl ether (200 mL) was added a diethyl ether solution of Me_2Mg (16.0 mL, 4.65 mmol) dropwise over 40 min. After the mixture was stirred overnight, the volatile materials

(62) Tessier-Youngs, C.; Beachley, O. T. *Inorg. Synth.* **1984**, *24*, 95.
(63) Coates, G. E.; Heslop, J. A. *J. Chem. Soc. A* **1968**, 514.
(64) Andersen, R. A.; Wilkinson, G. *J. Chem. Soc., Dalton Trans.* **1977**, 809.

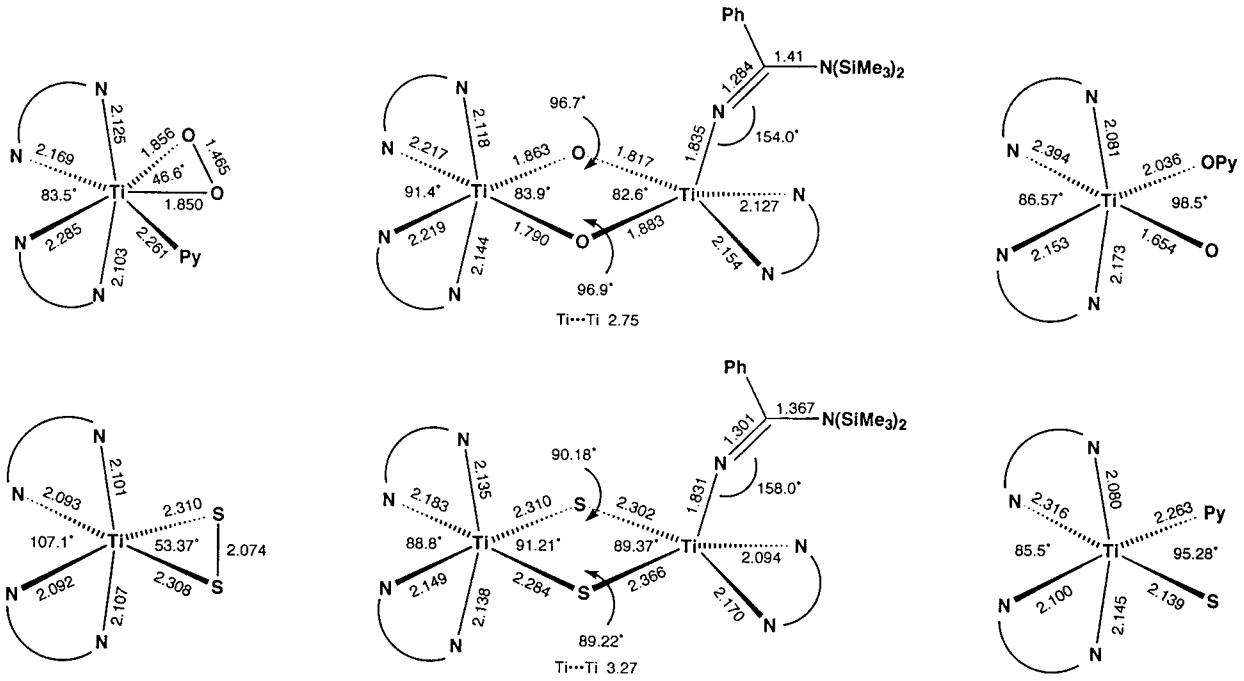

Figure 8. Comparison of the core structures.

Table 5. Selected Bond Distances (Å) and Angles (deg) for $L_2Ti(\eta^2\text{-}S_2)$

Ti(1)−S(1)	2.308(2)	Ti(2)−S(3)	2.317(2)
Ti(1)−S(2)	2.310(2)	Ti(2)−S(4)	2.312(2)
Ti(1)−N(1)	2.101(4)	Ti(2)−N(5)	2.111(4)
Ti(1)−N(2)	2.093(4)	Ti(2)−N(6)	2.101(4)
Ti(1)−N(3)	2.107(4)	Ti(2)−N(7)	2.100(4)
Ti(1)−N(4)	2.092(4)	Ti(2)−N(8)	2.090(4)
S(1)−S(2)	2.074(2)	S(3)−S(4)	2.075(2)
S(1)−Ti(1)−S(2)	53.37(6)	S(3)−Ti(2)−S(4)	53.25(5)
S(1)−Ti(1)−N(1)	102.3(1)	S(3)−Ti(2)−N(5)	102.7(1)
S(1)−Ti(1)−N(2)	151.9(1)	S(3)−Ti(2)−N(6)	156.3(1)
S(1)−Ti(1)−N(3)	99.7(1)	S(3)−Ti(2)−N(7)	98.9(1)
S(1)−Ti(1)−N(4)	99.6(1)	S(3)−Ti(2)−N(8)	95.6(1)
S(2)−Ti(1)−N(1)	100.6(1)	S(4)−Ti(2)−N(5)	100.3(1)
S(2)−Ti(1)−N(2)	102.4(1)	S(4)−Ti(2)−N(6)	107.1(1)
S(2)−Ti(1)−N(3)	102.0(1)	S(4)−Ti(2)−N(7)	100.3(1)
S(2)−Ti(1)−N(4)	149.3(1)	S(4)−Ti(2)−N(8)	144.6(1)
N(1)−Ti(1)−N(2)	65.2(1)	N(5)−Ti(2)−N(6)	64.9(1)
N(1)−Ti(1)−N(3)	155.0(2)	N(5)−Ti(2)−N(7)	156.3(1)
N(1)−Ti(1)−N(4)	99.5(1)	N(5)−Ti(2)−N(8)	103.0(1)
N(2)−Ti(1)−N(3)	99.5(1)	N(6)−Ti(2)−N(7)	97.8(1)
N(2)−Ti(1)−N(4)	107.1(2)	N(6)−Ti(2)−N(8)	106.8(1)
N(3)−Ti(1)−N(4)	64.9(1)	N(7)−Ti(2)−N(8)	65.1(1)

were removed under reduced pressure. The resulting red-brown paste was extracted with CH_2Cl_2 (100 mL). Filtration through a Celite pad on a fritted disk followed by concentration to 40 mL and cooling to −40 °C gave the product as analytically pure large red crystals (1.7 g, 60%). Mp: 151−155 °C. ^{1}H NMR (C_6D_6, 300 MHz): δ 7.30−7.25 (m, 4H), 7.05−7.00 (m, 6H), 1.96 (s, 6H), 0.15 (s, 36H). $^{13}C\{^1H\}$ NMR (C_6D_6, 75.5 MHz): δ 184.0, 140.7, 128.8, 128.3, 126.2, 69.1, 2.4. IR: 1427 (s), 1261 (m), 1247 (m), 1127 (w), 976 (s), 920 (w), 840 (s, br), 788 (m), 759 (m), 740 (m), 715 (m), 702 (m), 523 (m) cm^{-1}. Anal. Calcd for $C_{28}H_{52}N_4Si_4Ti$: C, 55.59; H, 8.66; N, 9.26. Found: C, 55.57; H, 8.39; N, 9.38.

$L_2Ti(CH_2Ph)_2$. Toluene (100 mL) was added to L_2TiCl_2 (5.00 g, 7.74 mmol) forming an orange-red solution. After the mixture was cooled to −78 °C, an Et_2O solution of $PhCH_2MgCl$ (9.86 mL, 15.5 mmol) was added dropwise over 5 min. The flask was shielded from light and allowed to warm to ambient temperature over a 5 h, forming a purple solution. After the mixture was stirred for an additional 2 h, the volatile materials were removed under reduced pressure. The dark solid was extracted with Et_2O (150 mL) and filtered. Cooling of the Et_2O extract to −30 °C afforded 1.38 g of product as dark purple crystals. The dark solid, which did not extract into the Et_2O, was extracted with toluene (45 mL) and filtered. Cooling of the toluene extract to −30 °C yielded 1.18 g of product as small, dark purple crystals. Total yield: 44%. Mp: 126−127 °C. ^{1}H NMR (C_6D_6, 300 MHz): δ 7.45 (d, J = 7.1 Hz, 4H), 7.31 (t, J = 7.6 Hz, 4H), 7.2−6.9 (m, 12H), 3.90 (br, 2H), 3.09 (br, 2H), 0.02 (s, 36H). $^{13}C\{^1H\}$ NMR (C_6D_6, 75.5 MHz): δ 187.1, 154.0, 140.6, 129.1, 128.6, 128.3, 127.3, 121.9, 105.5, 3.9, 2.5. IR: 3064 (w), 1594 (m), 1450 (vs, br), 1247 (s), 1207 (m), 1157 (w), 1075 (w), 1029 (w), 995 (m), 975 (s), 920 (w), 840 (vs), 787 (m), 741 (m), 712 (m), 546 (w), 503 (m) cm^{-1}. Anal. Calcd for $C_{40}H_{60}N_4Si_4Ti$: C, 63.45; H, 7.99; N, 7.40. Found: C, 63.34; H, 8.04; N, 7.22.

Table 6. Selected Bond Distances (Å) and Angles (deg) for $L_2Ti(\mu\text{-}S)_2TiL[\eta^1\text{-}NC(Ph)N(SiMe_3)_2]$

Ti(1)−S(1)	2.310(1)	Ti(1)−S(2)	2.284(1)
Ti(1)−N(1)	2.138(3)	Ti(1)−N(2)	2.149(3)
Ti(1)−N(3)	2.183(3)	Ti(1)−N(4)	2.135(3)
Ti(2)−S(1)	2.302(1)	Ti(2)−S(2)	2.366(1)
Ti(2)−N(5)	2.170(3)	Ti(2)−N(6)	2.094(3)
Ti(2)−N(7)	1.831(4)	Si(7)−N(8)	1.809(4)
Si(8)−N(8)	1.794(4)	N(1)−C(7)	1.337(5)
N(2)−C(7)	1.329(5)	N(3)−C(20)	1.329(5)
N(4)−C(20)	1.332(5)	N(5)−C(33)	1.335(5)
N(6)−C(33)	1.330(5)	N(7)−C(46)	1.301(5)
N(8)−C(46)	1.367(5)		
S(1)−Ti(1)−S(2)	91.21(5)	S(1)−Ti(1)−N(1)	92.8(1)
S(1)−Ti(1)−N(2)	155.7(1)	S(1)−Ti(1)−N(3)	91.34(9)
S(1)−Ti(1)−N(4)	104.8(1)	S(2)−Ti(1)−N(1)	103.7(1)
S(2)−Ti(1)−N(2)	98.0(1)	S(2)−Ti(1)−N(3)	157.0(1)
S(2)−Ti(1)−N(4)	94.4(1)	N(1)−Ti(1)−N(2)	63.3(1)
N(1)−Ti(1)−N(3)	99.0(1)	N(1)−Ti(1)−N(4)	154.5(1)
N(2)−Ti(1)−N(3)	88.8(1)	N(2)−Ti(1)−N(4)	96.9(1)
N(3)−Ti(1)−N(4)	62.9(1)	S(1)−Ti(2)−S(2)	89.37(5)
S(1)−Ti(2)−N(5)	142.4(1)	S(1)−Ti(2)−N(6)	141.5(1)
S(1)−Ti(2)−N(7)	105.1(1)	S(2)−Ti(2)−N(5)	87.9(1)
S(2)−Ti(2)−N(6)	141.5(1)	S(2)−Ti(2)−N(7)	113.4(1)
N(5)−Ti(2)−N(6)	63.8(1)	N(5)−Ti(2)−N(7)	110.3(1)
N(6)−Ti(2)−N(7)	101.2(1)	Ti(1)−S(1)−Ti(2)	90.18(5)
Ti(1)−S(2)−Ti(2)	89.22(5)	Ti(2)−N(7)−C(46)	158.0(3)
Si(7)−N(8)−Si(8)	122.0(2)	Si(7)−N(8)−C(46)	113.9(3)
Si(8)−N(8)−C(46)	123.6(3)	N(7)−C(46)−N(8)	123.4(4)

$L_2TiNCMe_3$. To a 100-mL round-bottomed flask charged with L_2TiMe_2 (2.25 g, 3.72 mmol) and benzene (50 mL) was added *tert*-butylamine (0.41 mL, 3.9 mmol). The mixture was heated to reflux overnight, then the volatiles were removed under reduced pressure. The resulting red solid was extracted with hexanes (50 mL) and filtered. Concentration to 25 mL and cooling to −40 °C gave the product as large orange crystals (1.04 g, 43.3%). Mp: 156−158 °C. ^{1}H NMR (C_6D_6, 300 MHz): δ 7.38−7.33 (m, 4H), 7.07−7.03 (m, 6H), 1.33 (s, 9H), 0.20 (s, 36H). ^{13}C{^{1}H} NMR (C_6D_6, 75.5 MHz): δ 180.8, 141.2, 129.0, 128.2, 127.7, 70.8, 33.5, 3.2. IR: 1437 (s), 1408 (s), 1246 (s), 1208 (w), 1168 (w), 1211 (w), 1002 (sh), 987 (m), 922 (w), 843 (s, br), 787 (w), 760 (m), 720 (w), 702 (w), 509 (m) cm^{-1}. Anal. Calcd for $C_{30}H_{55}N_5Si_4Ti$: C, 55.78; H, 8.58; N, 10.84. Found: C, 55.70; H, 8.61; N, 10.70.

$L_2TiCl(THF)\cdot 0.5(pentane)$. A 100-mL round-bottomed flask was charged with L_2TiCl_2 (1.00 g, 1.55 mmol) and 1% Na/Hg (0.071 g Na, 3.10 mmol). At −78 °C, tetrahydrofuran (35 mL) was added and the solution was allowed to warm to room temperature. After the mixture was stirred overnight, the volatiles were removed under reduced pressure. The resulting red-brown oil was extracted with pentane (50 mL) and filtered. Concentration to 15 mL followed by cooling to −40 °C gave the product as forest green flakes (0.30 g, 27%). Mp: 107−108 °C. ^{1}H NMR (C_6D_6, 300 MHz): δ 8.73 (br, 8H), 7.56 (br, 4H), 7.20 (br, 2H), 3.57 (br, 4H), 1.2 (m, 3H, pentane), 0.86 (t, 3H, pentane), 0.53 (br, 36H). IR: 1499 (w), 1245.3 (s), 1167 (w), 1074 (w), 1007 (m), 979 (s), 920 (w), 844 (s, br), 784 (w), 756 (m), 723 (w), 702 (w), 690 (w), 500 (m) cm^{-1}. Anal. Calcd for $C_{32.5}H_{60}ClN_4OSi_4Ti$: C, 54.33; H, 8.42; N, 7.80. Found: C, 54.06; H, 8.66; N, 7.70. $\mu_{eff} = 1.6\ \mu_B$.

L_2TiCl. A 100-mL round-bottomed flask was charged with L_2TiCl_2 (2.00 g, 3.10 mmol) and 1% Na/Hg (0.142 g Na, 6.19 mmol). Toluene (45 mL), cooled to −78 °C, was added, and the solution was allowed to warm slowly to room temperature. After the mixture was stirred overnight, the volatiles were removed under reduced pressure. The resulting red-gray residue was extracted with pentane (100 mL) and filtered. Concentration to 40 mL followed by cooling to −40 °C gave the product as dark red crystals. Total yield from two crops: 1.1 g, 57%. Mp: 174−175 °C. ^{1}H NMR (C_6D_6, 300 MHz): δ 10.42 (br, 4H), 8.49 (br, 4H), 7.63 (br, 2H), 1.28 (br, 36H). IR: 1600 (w), 1500 (m), 1247 (s), 1168 (w), 1074 (w), 1030 (w), 982 (s), 921 (w), 837 (s, br), 786 (m), 760 (s), 726 (m), 702 (m), 524 (m), 504 (sh) cm^{-1}. Anal. Calcd for $C_{26}H_{46}ClN_4Si_4Ti$: C, 51.16; H, 7.60; N, 9.18. Found: C, 50.83; H, 7.72; N, 9.06. $\mu_{eff} = 1.6\ \mu_B$.

$L_2TiCH_2SiMe_3$. To a 100-mL round-bottomed flask charged with $(L_2TiCl)_2$ (0.75 g, 0.61 mmol) and $LiCH_2SiMe_3$ (0.116 g, 1.22 mmol) was added toluene (20 mL), forming a clear dark red solution. After the mixture was stirred overnight, the volatile materials were removed under reduced pressure. The resulting dark red residue was extracted with hexanes (40 mL) and filtered. The hexanes were then removed under reduced pressure and HMDSO (15 mL) was added. Concentration to 3 mL and cooling to −40 °C gave the product as red crystals (0.52 g, 64%). Mp: 110−112 °C. ^{1}H NMR (C_6D_6, 300 MHz): δ 10.82 (br, 4H), 8.36 (br, 4H), 7.77 (br, 2H), 0.95 (br, 36H), 0.10 (br, 9H). IR: 1260 (sh), 1247 (s), 1168 (w), 1073 (w), 983 (s), 917 (w), 844 (s, br), 785 (w), 759 (m), 721 (w), 701 (m), 604 (w), 518 (m) cm^{-1}. Anal. Calcd for $C_{30}H_{57}N_4Si_5Ti$: C, 54.42; H, 8.68; N, 8.46. Found: C, 54.09; H, 8.63; N, 8.48. $\mu_{eff} = 1.6\ \mu_B$.

L_2TiMe. Tetrahydrofuran (40 mL) was added to $L_2Ti(Me)$-Cl (3.25 g, 5.20 mmol) and Na/Hg (0.48 g Na, 20.8 mmol) in a 100-mL round-bottomed flask. After the mixture was stirred overnight, the volatile materials were removed under reduced pressure. The red-brown solid was extracted with hexanes (80 mL) and filtered through a Celite pad on a fritted disk. The volatiles were removed under reduced pressure, and the residue was evacuated overnight to remove any remaining THF. The residue was taken up in HMDSO and concentrated to 20 mL. Cooling to −40 °C yielded red crystals (2.1 g, 69%) of product. Recrystallization from HMDSO gave analytically pure product. Mp: 120−122 °C. ^{1}H NMR (C_6D_6, 300 MHz): δ 10.93 (br, 4H), 8.48 (br, 4H), 7.77 (br, 2H), 1.21 (br, 36H). IR: 1498 (m), 1448 (s, br), 1284 (s, br), 1258 (sh), 1245 (s), 1170 (w), 1094 (w), 1073 (w), 1032 (w), 1002 (sh), 982 (s), 917 (m), 844 (s, br), 785 (m), 758 (s), 718 (m), 701 (m), 682 (m), 604 (w), 533 (m), 505 (m) cm^{-1}. Anal. Calcd for $C_{27}H_{49}N_4OSi_4Ti$: C, 54.97; H, 8.37; N, 9.50. Found: C, 54.64; H, 8.55; N, 9.27. $\mu_{eff} = 1.6\ \mu_B$.

$(L_2Ti)_2(\mu\text{-}N_2)$. To a 500-mL round-bottomed flask containing L_2TiCl_2 (15.0 g, 23.3 mmol) and Na/Hg (4.45 g Na, 190 mmol) was added toluene (250 mL). After the mixture was stirred for 3 days, a dark blue-black solution had formed. The volatile materials were removed under reduced pressure. The resulting black solid was extracted with warm toluene (150 mL) and filtered through Celite on a fritted disk. Concentration of the dark blue solution to 100 mL and cooling to −30 °C gave the product as blue-black crystals. Total yield from 3 crops: 5.6 g, 41%. Mp: 268 °C (dec). ^{1}H NMR (C_6D_6, 300 MHz): δ 7.56 (br, 4H), 7.15−7.08 (m, 6H), 0.22 (br, 36H). ^{13}C-{^{1}H} NMR (C_6D_6, 75.5 MHz): δ 178.3, 141.6, 129.1, 127.7, 2.9 (br). IR: 1305 (w, br), 1259 (sh), 1246 (s), 1170 (w), 1074 (w), 1031 (w), 1002 (sh), 984 (s), 920 (w), 844 (s, br), 786 (w), 763 (m), 721 (w), 700 (w), 604 (w), 509 (m), 495 (sh) cm^{-1}. Anal. Calcd for $C_{52}H_{92}N_{10}Si_8Ti_2$: C, 53.03; H, 7.87; N, 11.89. Found: C, 52.74; H, 7.85; N, 11.91.

$(L_2Ti)_2(\mu\text{-}O)$. Manipulations were carried out under argon. Toluene (100 mL) was added to a 250-mL round-bottomed flask containing L_2TiCl_2 (2.00 g, 3.10 mmol) and Na/Hg (0.71 g Na, 31 mmol). The flask was briefly evacuated and then backfilled with CO. After the mixture was stirred for 2 days, the volatile materials were removed under reduced pressure. The resulting black solid was extracted with hexanes (100 mL) and filtered through a pad of Celite on a fritted disk. Concentration to 30 mL and cooling to −40 °C gave the product as red-black crystals (0.38 g, 18%). Mp: 275 °C (dec). ^{1}H NMR (C_6D_6, 300 MHz): δ 10.0 (v br), 7.58 (br, 4H), 6.65 (br, 2H), 2.0−0.2 (50H). IR: 1407 (s), 1259 (sh), 1248 (s), 1172 (w), 982 (s), 918 (w), 848 (s, br), 791 (s), 761 (s), 721 (m), 700 (m), 605 (w), 510 (m) cm^{-1}. Anal. Calcd for $C_{64}H_{120}N_8OSi_8Ti_2$: C, 53.57; H, 7.95; N, 9.61. Found: C, 53.20; H, 8.16; N, 9.51. $\mu_{eff} = 2.4\ \mu_B$. EI-MS 1165 (M^+) (correct isotope pattern was observed).

$(L_2Ti)_2(\mu\text{-}^{18}O)$. The above reaction was carried out on a one-half scale using $C^{18}O$ (95% ^{18}O). Mp: 275 °C (dec). EI-MS 1167 (M^+) (correct isotope pattern for the ^{18}O incorporated product was observed).

Reduction of L_2TiCl_2 in the Presence of TMEDA. All manipulations were carried out under Ar. Toluene (40 mL) and TMEDA (2.3 mL, 16 mmol) were added to a 100-mL round-bottomed flask containing L_2TiCl_2 (1.00 g, 1.55 mmol) and Na/Hg (0.21 g Na, 9.2 mmol). After the mixture was stirred overnight, the volatiles were removed under reduced pressure. The purple-brown residue was extracted with hexanes (40 mL) and filtered through a Celite pad on a fritted disk. Concentration to 3 mL and cooling to −40 °C yielded yellow crystals (0.25 g, 24% based on Ti) of $L_2TiNSiMe_3$. Concentration of the mother liquor to 2 mL and cooling to −40 °C yielded red-black crystals (0.39 g, 42% based on Ti) of $LTi[\eta^2\text{-}Me_3SiNC(H)Ph][\eta^3\text{-}CH_2N(Me)CH_2CH_2N(Me)_2]$. Recrystallization of both products from hexanes yielded analytically pure samples. **$L_2TiNSiMe_3$:** Mp 162−163 °C; ^{1}H NMR (C_6D_6, 300 MHz) δ 7.37−7.31 (m, 4H), 7.05−6.98 (m, 6H), 0.29 (s, 9H), 0.20 (s, 36H); ^{13}C{^{1}H} NMR (C_6D_6, 75.5 MHz) δ 181.8, 140.6, 129.4, 128.2, 3.8, 2.9; MS (EI) *m*/*z* (relative intensity) 661 (M^+, 87), 572 (20), 558 (10), 543 (20), 399 (53), 304 (10), 280 (10), 263 (12), 247 (10), 176 (57), 73 (100); IR 1425 (s, br), 1245 (s), 1166 (w), 1111 (s), 1074 (sh), 1030 (m), 1002 (m), 986 (s), 926 (w), 842 (s, br), 789 (m), 757 (s), 701 (m), 637 (w), 603 (w), 511 (m) cm^{-1}. Anal. Calcd for $C_{29}H_{55}N_5Si_5Ti$: C, 52.61; H, 8.37; N,

10.58. Found: C, 52.41; H, 8.43; N, 10.40. **LTi[η^2-Me$_3$SiNC(H)Ph][η^3-CH$_2$N(Me)CH$_2$CH$_2$N(Me)$_2$]:** Mp 101−103 °C; ^{1}H NMR (C_6D_6, 300 MHz, 90 °C): δ 7.43−7.38 (m, 2H), 7.30−7.24 (m, 2H), 7.13 (m, 1H), 7.08−7.01 (m, 3H), 6.94−6.85 (m, 1H), 5.49 (s, 1H), 3.09 (br, 2H), 2.74 (br, 3H), 2.61−2.55 (m, 2H), 2.36 (br, 2H), 2.13 (s, 6H), 0.29 (s, 9H), −0.03 (s, 9H), −0.29 (s, 9H); ^{13}C{^{1}H} NMR (C_6D_6, 75.5 MHz, 80 °C) δ 155.1, 140.5, 128.7, 128.1, 126.9, 122.4, 121.1, 111.8, 58.0, 56.1, 46.9, 45.8, 2.3, 2.0; IR 1587 (s), 1432 (s, br), 1377 (m), 1277 (w), 1244 (s), 1219 (m), 1169 (w), 1148 (w), 1126 (m), 1070 (m), 984 (s), 940 (w), 910 (w), 836 (s, br), 785 (w), 757 (m), 744 (m), 708 (m), 675 (w), 640 (w), 609 (w), 558 (w), 536 (m), 505 (m), 482 (m) cm^{-1}. Anal. Calcd for $C_{29}H_{53}N_5Si_3Ti$: C, 57.68; H, 8.85; N, 11.60. Found: C, 57.81; H, 9.05; N, 11.48.

[L$_2$Ti(Py)]$_2$(μ-N$_2$). Pyridine (74 μL, 0.91 mmol) was added to a dark blue solution of (L$_2$Ti)$_2$(μ-N$_2$) (0.27 g, 0.23 mmol) in toluene (20 mL). Immediately, a deep red solution formed. After the mixture was stirred overnight, the volatile materials were removed under reduced pressure, affording a red solid. The solid was extracted with hot hexanes (50 mL) and filtered. Cooling to −30 °C gave the product as red blocks. Total yield from 2 crops: 0.132 g, 43.3%. Mp: 142 °C (dec). ^{1}H NMR (C_6D_6, 300 MHz, 60 °C): δ 9.10 (v br, 4H), 7.43 (br, 8H), 7.15−6.90 (m), 0.20 (s, 72H). IR: 1602 (w), 1498 (m), 1460 (br, vs), 1376 (s), 1244 (m), 1166 (w), 1071 (w), 981 (s), 922 (w), 842 (br, s), 784 (w), 757 (m), 702 (m), 494 (m) cm^{-1}. Anal. Calcd for $C_{62}H_{102}N_{12}Si_8Ti_2$: C, 55.74; H, 7.69; N, 12.58. Found: C, 56.05; H, 7.83; N, 12.42.

[L$_2$Ti(CNXylyl)]$_2$(μ-N$_2$). Toluene (15 mL) was added to (L$_2$Ti)$_2$(μ-N$_2$) (0.26 g, 0.22 mmol) and XylylNC (57 mg, 0.43 mmol) forming a dark red solution. After 30 min, the volatile materials were removed under reduced pressure, affording a dark red solid. The solid was extracted with warm hexanes (30 mL) and filtered. Concentration to 20 mL and cooling to −30 °C gave the product as a rose solid (0.16 g, 50%). Mp: 137 °C (dec). ^{1}H NMR (C_6D_6, 300 MHz, 50 °C): δ 7.57 (m, 8H), 7.19−7.08 (m), 6.68 (br, 6H), 2.36 (br, 12H), 0.25 (s, 72H). IR: 2143 (s), 1510 (m), 1454 (br, vs), 1371 (s), 1360 (s), 1241 (m), 1169 (w), 1001 (w), 978 (s), 913 (w), 843 (br, s), 776 (m), 755 (m), 722 (w), 698 (w) cm^{-1}. Anal. Calcd for $C_{70}H_{110}N_{12}Si_8Ti_2$·hexane: C, 59.80; H, 8.19; N, 11.01. Found: C, 60.01; H, 8.24; N, 10.97.

L$_2$Ti(η^2-O$_2$)Py. Pyridine (1 mL) was added to a hexanes solution (20 mL) of (L$_2$Ti)$_2$(μ-N$_2$) (0.35 g, 0.30 mmol) forming a dark red solution. The flask was evacuated briefly and then backfilled with dry O_2 (2 psig). Within 20 s, a clear orange solution had formed. After 2 min, the volatile materials were removed under reduced pressure, giving an orange solid (0.28 g, 69%). The product can be crystallized from Et$_2$O in ca. 40% yield. Mp: 128−132 °C. ^{1}H NMR (C_6D_6, 300 MHz): δ 9.17 (d, 2H), 7.24 (m, 4H), 7.01 (m, 6H), 6.93 (t, 1H), 6.61 (t, 2H), 0.12 (s, 36H). IR: 1601 (m), 1501 (m), 1461 (vs, br), 1384 (s, br), 1244 (s), 1216 (w), 1168 (w), 1151 (w), 1073 (w), 1040 (w), 1008 (w), 981 (s), 887 (s), 842 (s, br), 792 (m), 758 (m), 743 (m), 720 (m), 701 (m), 633 (w), 613 (m), 573 (m), 500 (m) cm^{-1}. Anal. Calcd for $C_{31}H_{51}N_5O_2Si_4Ti$: C, 54.28; H, 7.49; N, 10.21. Found: C, 54.59; H, 7.60; N, 10.11.

L$_2$Ti(μ-O)$_2$TiL[η^1-NC(Ph)N(SiMe$_3$)$_2$]. A sample of (L$_2$Ti)$_2$(μ-N$_2$) (0.19 g, 0.16 mmol) was ground to a powder using a mortar and pestle. This blue powder was loaded into a Schlenk tube and evacuated. Upon filling the tube with dry O_2 (2 psig), the solid became a bright yellow. After 5 min, ^{1}H NMR spectroscopy of the sample (in C_6D_6) revealed it to be completely converted to the product (0.15 g, 79%). Mp: 225−229 °C. ^{1}H NMR (toluene-d_8, 300 MHz, 100 °C): δ 8.09 (d, 2H), 7.5−6.9 (m), 0.34 (s), 0.19 (br), 0.19 (s), 0.00 (br) (total 72 H for −SiMe$_3$ region). IR: 1575 (w), 1546 (s), 1499 (m), 1460 (vs, br), 1374 (s), 1243 (s, br), 1173 (w, br), 1122 (w), 1074 (w), 981 (m), 917 (w), 843 (vs, br), 765 (m), 722 (m), 677 (m), 651 (m), 613 (m), 595 (m), 504 (m), 487 (m) cm^{-1}. Anal. Calcd for $C_{52}H_{92}N_8O_2Si_8Ti_2$: C, 52.85; H, 7.85; N, 9.48. Found: C, 52.39; H, 7.84; N, 9.26.

L$_2$Ti(O)OPy. Hexanes (20 mL) and pyridine (1 mL) were added to (L$_2$Ti)$_2$(μ-N$_2$) (0.26 g, 0.22 mmol) forming a dark red solution. This solution was added to solid PyO (0.10 g, 1.1 mmol) in a 100-mL round-bottomed flask. Toluene (20 mL) was added to help dissolve the PyO. After the mixture was overnight, the volatile materials were removed under reduced pressure, affording a rose solid. The solid was extracted with Et$_2$O (30 mL) and filtered. Concentration to 20 mL and cooling to −30 °C afforded the product as pale lavender crystals (0.11 g, 37%). Recrystallization from Et$_2$O gave analytically pure colorless crystals. Mp: 167−169 °C (dec). ^{1}H NMR (C_6D_6, 300 MHz): δ 9.29 (br, 2H), 7.40 (m, 4H), 7.15−7.05 (m, 6H), 6.29 (t, 1H), 6.22 (t, 2H), 0.25 (s, 36H). IR: 1529 (s), 1460 (vs, br), 1435 (s), 1378 (s), 1242 (s), 1217 (s), 1167 (m), 1071 (w), 1010 (w), 981 (s), 929 (m), 909 (s), 841 (vs, br), 789 (m), 759 (s), 722 (m), 701 (m), 673 (w), 605 (w), 578 (m), 500 (m) cm^{-1}. Anal. Calcd for $C_{31}H_{51}N_5O_2Si_4Ti$: C, 54.28; H, 7.49; N, 10.21. Found: C, 54.22; H, 7.55; N, 10.11.

L$_2$Ti(η^2-S$_2$). Toluene (25 mL) was added to (L$_2$Ti)$_2$(μ-N$_2$) (0.21 g, 0.18 mmol) and S_8 (79 mg, 0.31 mmol) forming a dark blue solution. Within a few minutes, the solution became teal. After 45 min, the volatiles were removed under reduced pressure giving a teal solid. The solid was extracted with hexanes (35 mL). A small amount of pale solid was filtered off, likely unreacted sulfur. Upon concentration, more pale solid formed. The solution was then filtered again, concentrated to 10 mL, and cooled to −30 °C. The product was isolated as green-black blocks (0.14 g, 62%). An analytically pure sample was obtained by recrystallization from hexanes. Mp: 178−180 °C. ^{1}H NMR (C_6D_6, 300 MHz): δ 7.22−7.19 (m, 4H), 7.00−6.90 (m, 6H), 0.11 (s, 36H). IR: 1456 (vs, br), 1417 (s), 1399 (s), 1376 (s), 1258 (m), 1243 (s), 1163 (m, br), 1074 (w), 1031 (w), 1004 (m), 978 (s), 922 (w), 844 (vs, br), 784 (w), 763 (s), 745 (w), 707 (s), 668 (w), 522 (m), 513 (m) cm^{-1}. Anal. Calcd for $C_{26}H_{46}N_4S_2Si_4Ti$: C, 48.87; H, 7.26; N, 8.77. Found: C, 49.02; H, 7.34; N, 8.66.

L$_2$Ti(μ-S)$_2$TiL[η^1-NC(Ph)N(SiMe$_3$)$_2$]. Toluene (20 mL) was added to L$_2$Ti(η^2-S$_2$) (0.20 g, 0.31 mmol) and Hg (11 g) in a 100-mL round-bottomed flask, forming a teal solution. After the mixture was stirred for 17 h, the solution became red. The volatile materials were removed under reduced pressure. The solid was extracted with hexanes (35 mL) and filtered through Supercel on a fritted disk. The clear, orange-red solution was stripped to dryness, affording an orange solid (0.10 g, 53%). Crystallization from Et$_2$O yielded analytically pure product in ca. 20% yield. Mp: 228−230 °C. ^{1}H NMR ($CDCl_3$, 300 MHz): δ 8.17−8.12 (m, 2H), 7.41−7.25 (m, 18H), 0.25 (s, 18H), 0.24 (s, 9H), −0.08 (br, 18H), −0.16 (s, 9H), −0.30 (v br, 18H). IR: 1518 (s), 1459 (vs, br), 1377 (s), 1294 (m), 1281 (m), 1257 (w), 1243 (m), 1168 (w), 1143 (w), 1073 (w), 1030 (w), 1002 (m), 988 (m), 976 (m), 920 (w), 843 (s, br), 767 (m), 722 (m), 655 (w), 501 (m), 488 (w) cm^{-1}. Anal. Calcd for $C_{52}H_{92}N_8S_2Si_8Ti_2$: C, 51.45; H, 7.64; N, 9.23. Found: C, 51.36; H, 7.75; N, 9.21.

L$_2$Ti(S)Py. Mercury (15 g) was added to a dark green solution of L$_2$Ti(η^2-S$_2$) (0.32 g, 0.50 mmol), pyridine (0.40 g, 4.9 mmol), and toluene (25 mL). After the mixture was stirred overnight, the solution became orange-red. The volatile materials were removed under reduced pressure, and the solid was extracted with hexanes (40 mL). The solution was filtered through Supercel on a fritted disk, and the hexanes were removed under reduced pressure. Crystallization form Et$_2$O/hexanes at −30 °C yielded the product as small orange-red crystals (80 mg, 23%). Mp: 221−227 °C. ^{1}H NMR (C_6D_6, 300 MHz): δ 9.53 (br, 2H), 7.36 (m, 4H), 7.10−7.00 (m, 6H), 6.95 (br, 1H), 6.67 (br, 2H), 0.20 (s, 36H). IR: 1601 (m), 1499 (m), 1463 (vs, br), 1426 (s), 1379 (s), 1246 (s), 1215 (w), 1167 (w), 1068 (w), 1002 (w), 992 (w), 977 (s), 842 (s, br), 791 (w), 760 (m), 722 (m), 699 (w), 631 (w), 520 (m), 501 (m) cm^{-1}. Anal.

Table 7. Crystal Data and Collection Parameters (L = PhC(NSiMe$_3$)$_2$)

compd	$L_2TiNCMe_3$	L_2TiCl	$[L_2Ti(Py)]_2(\mu\text{-}N_2)$	$L_2Ti(O)OPy$	$L_2Ti(\eta^2\text{-}S_2)$	$L_2Ti(\mu\text{-}S)_2TiL[\eta^1\text{-}NC(Ph)N(SiMe_3)_2]$
formula	$C_{30}H_{55}N_5Si_4Ti$	$C_{26}H_{46}N_4Si_4TiCl$	$C_{62}H_{102}N_{12}Si_8Ti_2$	$C_{31}H_{51}N_5Si_4TiO_2$	$C_{26}H_{46}N_4Si_4TiS_2$	$C_{52}H_{92}N_8Si_8Ti_2S_2$
fw	689.36	610.37	1336.05	686.02	639.04	1213.96
space group	$P2_1/n$ (No. 14)	$P\bar{1}$ (No. 2)	Cc (No. 9)	$P2_1/c$ (No. 14)	$P2_1/n$ (No. 14)	$P\bar{1}$ (No. 2)
temp (°C)	−105	−142	−135	−99	−114	−93
a (Å)	11.438(3)	12.1926(4)	18.4660(4)	15.7453(1)	20.0421(4)	12.9999(2)
b (Å)	29.93(1)	12.7951(3)	14.3878(2)	11.5487(1)	15.7823(2)	14.076(2)
c (Å)	11.530(4)	13.1292(5)	29.4826(6)	21.7934(2)	24.1409(5)	20.9523(1)
V (Å^3)	3847(2)	1708.1(2)	7529.0(4)	3824.47(5)	7109.1(3)	3446.2(1)
α (deg)		66.031(1)				105.438(1)
β (deg)	102.93(2)	74.957(1)	106.019(1)	105.186(1)	111.409(1)	104.062(1)
γ (deg)		66.799(1)				100.199(1)
Z	4	2	4	4	8	2
d_{calc} (g/cm^3)	1.116	1.187	1.179	1.191	1.194	1.170
diffractometer	Enraf-Nonius CAD−4	Siemens SMART	Siemens SMART	Siemens SMART	Siemens SMART	Siemens SMART
radiation	Mo Kα (λ = 0.710 73 Å)	Mo Kα (λ = 0.710 73 Å)	Mo Kα (λ = 0.710 73 Å)	Mo Kα (λ = 0.710 73 Å)	Mo Kα (λ = 0.710 73 Å)	Mo Kα (λ = 0.710 73 Å)
monochromator	graphite	graphite	graphite	graphite	graphite	graphite
detector	crystal scintillation counter	CCD area detector	CCD area detector	CCD area detector	CCD area detector	CCD area detector
scan type, width	θ−2θ, $\Delta\theta$ = 0.70 + 0.35 tan θ	ω, 0.3°	ω, 0.3°	ω, 0.3°	ω, 0.3°	ω, 0.3°
scan speed	5.49 (θ, deg/min)	30 s/frame	30 s/frame	10 s/frame	10 s/frame	20 s/frame
reflections measured	$-h,-k,\pm l$	hemisphere	hemisphere	hemisphere	hemisphere	hemisphere
2θ range (deg)	3−45	3−46.5	3−46.5	3−46.5	3−46.5	3−46.5
μ (mm^{-1})	0.372	0.490	0.383	0.382	0.514	0.469
T_{min}, T_{max}	0.86, 1.00	0.825, 0.985	0.848, 0.917	0.771, 0.942	0.763, 0.966	0.797, 0.977
cryst dimens (mm)	0.70 × 0.60 × 0.40	0.17 × 0.11 × 0.07	0.15 × 0.13 × 0.04	0.40 × 0.23 × 0.21	0.39 × 0.14 × 0.12	0.41 × 0.07 × 0.07
no. of reflns measd	5759	8198	15 878	15 692	29 535	14 503
no. of unique reflns	5298	5725	7706	5767	10 577	9671
no. of observations	3618	3946	6086	3737	5066	6127
no. of params	359	325	755	388	667	649
R, R_w (%)	11.3, 12.8	4.11, 4.82	3.45, 4.00	3.51, 4.16	3.69, 3.94	4.20, 4.56
GOF	5.850	1.426	1.293	1.426	1.142	1.331

Calcd for $C_{31}H_{51}N_5SSi_4Ti$: C, 54.27; H, 7.49; N, 10.21. Found: C, 54.26; H, 7.57; N, 10.11.

X-ray Crystallography. Table 7 lists a summary of crystal data and collection parameters for all structurally characterized compounds. Specific details of individual data collection and solution are given below.

$L_2TiNCMe_3$. Crystals suitable for X-ray diffraction studies were grown from hexanes at −20 °C. A large crystal was cut to the appropriate size (0.70 × 0.60 × 0.40 mm) and mounted[65] on a glass fiber using Paratone-N hydrocarbon oil. The crystal was transferred to an Enraf-Nonius CAD-4 diffractometer, centered in the beam, and cooled to −105 °C by a nitrogen-flow low-temperature apparatus, which had been previously calibrated by a thermocouple placed at the same position as the crystal. Automatic peak search and indexing procedures yielded a primitive monoclinic cell.

The 5694 raw intensity data were converted to structure factor amplitudes and their esd's by correction for scan speed, background, and Lorentz and polarization effects. Inspection of intensity standards revealed an overall decay of 36%. The data were corrected for this decay. Inspection of the azimuthal scan data[66] showed a variation I_{min}/I_{max} = 0.86 for the average curve. An empirical correction was applied to the data using DIFABS. Inspection of the systematic absences uniquely indicated space group $P2_1/n$ (No. 14). Removal of the systematically absent and averaging of redundant data (R_{int} = 16.8%) left 5298 unique reflections in the final data set. The structure was solved and refined with the teXsan[67] software package using direct methods[68] and expanded using Fourier techniques.[69] Disorder in the *tert*-butyl group was modeled as one-half occupancy in two positions, leading to four one-half-occupancy carbon atoms (C(1A), C(1B), C(2A), C(2B)), which were refined isotropically. All remaining non-hydrogen atoms were refined anisotropically. Hydrogen atoms were assigned idealized positions (not included for *tert*-butyl group) and were included in structure factor calculations but were not refined. The *p*-factor, used to reduce the weight of intense reflections, was set to 0.030 throughout the refinement. The analytical forms of the scattering factor tables for the neutral atoms were used,[70] and all scattering factors were corrected for both the real and imaginary components of anomalous dispersion.[71]

L_2TiCl. Crystals suitable for X-ray diffraction studies were grown over several days at −30 °C from hexanes solution. A

(65) Hope, H. *Experimental Organometallic Chemistry*; Wayda, A. L., Darensbourg, M. Y., Eds.; American Chemical Society, Conference Proceedings; Washington, DC, 1987; Vol. 357, p 257.

(66) Reflections used for azimuthal scans were located near χ = 90°, and the intensities were measured at 10° increments of rotation of the crystal about the diffraction vector.

(67) *teXsan: Crystal Structure Analysis Package*; Molecular Structure Corp.: The Woodlands, TX, 1992.

(68) Hai-Fu, F. *Structure Analysis Programs with Intelligent Control*; Hai-Fu, F., Ed.; Rigaku Corp.: Tokyo, 1991.

(69) Beurskens, P. T.; Admiraal, G.; Beuskens, G.; Bosman, W. P.; Garcia-Granda, S.; Gould, R. O.; Smits, J. M. M.; Smkalla, C. *DIRDIF92: The DIRDIF Program System*; Technical Report of the Crystallography Laboratory; Beurskens, P. T., Admiraal, G., Beuskens, G., Bosman, W. P., Garcia-Granda, S., Gould, R. O., Smits, J. M. M., Smkalla, C., Eds.; University of Nijmegen: Nijmegen, The Netherlands, 1992.

(70) Cromer, D. T.; Waber, J. T. In *International Tables for X-ray Crystallography*; The Kynoch Press: Birmingham, England, 1974; Vol. IV, Table 2.2B.

(71) Cromer, D. T.; Waber, J. T. In *International Tables for X-ray Crystallography*; The Kynoch Press: Birmingham, England, 1974; Vol. IV, Table 2.3.1.

large crystal was cut to the appropriate size (0.17 × 0.11 × 0.07 mm) and mounted as above. The crystal was transferred to a Siemens SMART diffractometer/CCD area detector,[72] centered in the beam, and cooled to −142 °C by a nitrogen flow low-temperature apparatus, which had been previously calibrated by a thermocouple placed at the same position as the crystal. Preliminary orientation matrix and cell constants were determined by collection of 60 10-s frames, followed by spot integration and least-squares refinement. A hemisphere of data was collected using 0.3° ω scans at 30 s per frame. The raw data were integrated (xy spot spread = 1.60°; z spot spread = 0.60°) and the unit cell parameters refined (4311 reflections with $I > 10\sigma(I)$) using SAINT.[73] Data analysis was performed using XPREP.[74] Absorption correction was applied using SADABS (T_{min} = 0.825, T_{max} = 0.985).[75] The unit cell parameters indicated a triclinic cell. The choice of the centric space group was confirmed by the successful refinement of the model. The data were corrected for Lorentz and polarization effects, but no correction for crystal decay was applied.

The 8198 reflections measured were averaged (R_{int} = 2.45%), yielding 7706 unique reflections. The structure was solved and refined with the teXsan[67] software package using direct methods[68] and expanded using Fourier techniques.[69] All non-hydrogen atoms were refined anisotropically. Hydrogen atoms were assigned idealized positions and were included in structure factor calculations but were not refined.

$[L_2Ti(Py)]_2(\mu\text{-}N_2)$. Crystals suitable for X-ray diffraction studies were grown over several days at −40 °C from hexanes solution. A large crystal was cut to the appropriate size (0.15 × 0.13 × 0.04 mm) and mounted as above. Data collection, integration, analysis, and processing were carried out analogously to that described for L_2TiCl. The unit cell parameters indicated a C-centered monoclinic cell; systematic absences were consistent with $C2/c$ (No. 15) and Cc (No. 9). The choice of the acentric space group was confirmed by the successful refinement of the model. The data were corrected for Lorentz and polarization effects, but no correction for crystal decay was applied.

The 15 878 reflections measured were averaged (R_{int} = 4.54%), yielding 7706 unique reflections. The structure was solved and refined with the teXsan[67] software package using direct methods[68] and expanded using Fourier techniques.[69] All non-hydrogen atoms were refined anisotropically. Hydrogen atoms were assigned idealized positions and were included in structure factor calculations but were not refined. The Flack parameter refined to 0.0442, indicating that the correct absolute structure was used.

$L_2Ti(O)OPy$. Crystals suitable for X-ray diffraction studies were grown over several days at −40 °C from Et_2O. A crystal of the appropriate size (0.40 × 0.23 × 0.21 mm) was mounted as above. Data collection, integration, analysis, and processing were carried out analogously to that described for L_2TiCl. The unit cell parameters indicated a primitive monoclinic cell; systematic absences indicated space group $P2_1/c$ (No. 14). The data were corrected for Lorentz and polarization effects, but no correction for crystal decay was applied.

The 15 692 reflections measured were averaged (R_{int} = 3.30%), yielding 5767 unique reflections. The structure was solved and refined with the teXsan software package using direct methods and expanded using Fourier techniques. All non-hydrogen atoms were refined anisotropically. Hydrogen atoms were assigned idealized positions and were included in structure factor calculations but were not refined.

$L_2Ti(\eta^2\text{-}S_2)$. Crystals suitable for X-ray diffraction studies were grown over several days at −40 °C from hexanes. A large crystal was cut to the appropriate size (0.39 × 0.14 × 0.12 mm) and mounted on a quartz capillary using Paratone-N hydrocarbon oil. Data collection, integration, analysis, and processing were carried out analogously to that described for L_2TiCl. The unit cell parameters indicated a primitive monoclinic cell; systematic absences indicated space group $P2_1/n$ (No. 14). The data were corrected for Lorentz and polarization effects, but no correction for crystal decay was applied.

The 29 535 reflections measured were averaged (R_{int} = 5.63%), yielding 10 577 unique reflections. The structure was solved and refined with the teXsan software package using direct methods and expanded using Fourier techniques. All non-hydrogen atoms were refined anisotropically. Hydrogen atoms were assigned idealized positions and were included in structure factor calculations but were not refined.

$L_2Ti(\mu\text{-}S)_2TiL[\eta^1\text{-}NC(Ph)N(SiMe_3)_2]$. Crystals suitable for X-ray diffraction studies were grown over several days at 25 °C from Et_2O. A crystal was cut to the appropriate size (0.41 × 0.07 × 0.07 mm) and mounted as above. Data collection, integration, analysis, and processing were carried out analogously to that described for L_2TiCl. The unit cell parameters indicated a triclinic cell; the choice of the centric space group $P\bar{1}$ (No. 2) was confirmed by the successful refinement of the structure. The data were corrected for Lorentz and polarization effects, but no correction for crystal decay was applied.

The 14 503 reflections measured were averaged (R_{int} = 2.95%), yielding 9671 unique reflections. The structure was solved and refined with the teXsan software package using direct methods and expanded using Fourier techniques. All non-hydrogen atoms were refined anisotropically. Hydrogen atoms were assigned idealized positions and were included in structure factor calculations but were not refined.

Acknowledgment. We thank the Petroleum Research Fund, administered by the American Chemical Society, for funding and the Sloan Foundation for the award of a fellowship to J.A.

Supporting Information Available: ORTEP views and tables of positional and thermal parameters and bond distances and angles for all crystallographically characterized compounds (49 pages). Ordering information is given on any current masthead page.

OM970933C

(72) *SMART: Area-Detector Software Package*; Siemens Industrial Automation, Inc.: Madison, WI, 1993.
(73) *SAINT: Area-Detector Integration Program*, 4.024 ed.; Siemens Industrial Automation, Inc.: Madison, WI, 1995.
(74) *XPREP: Part of the SHELXTL Crystal-Structure Determination Package*, 5.03 ed.; Siemens Industrial Automation: Madison, WI, 1994.
(75) *SADABS: Siemens Area-Detector Absorption Correction*; Siemens Industrial Automation, Inc.: Madison, WI, 1996.